

● Review

ULTRASOUND IMAGING TECHNOLOGIES FOR BREAST CANCER DETECTION AND MANAGEMENT: A REVIEW

RONGRONG GUO,^{*,†} GUOLAN LU,[‡] BINJIE QIN,[§] and BAOWEI FEI^{*,‡,¶,||}

^{*} Department of Radiology and Imaging Sciences, Emory University School of Medicine, Atlanta, Georgia, USA; [†] Department of Ultrasound, Shanxi Provincial Cancer Hospital, Taiyuan, Shanxi, China; [‡] The Wallace H. Coulter Department of Biomedical Engineering, Emory University and Georgia Institute of Technology, Atlanta, Georgia, USA; [§] School of Biomedical Engineering, Shanghai Jiao Tong University, Shanghai, China; [¶] Department of Mathematics and Computer Science, Emory College of Emory University, Atlanta, Georgia, USA; and ^{||} Winship Cancer Institute of Emory University, Atlanta, Georgia, USA

(Received 9 May 2017; revised 12 September 2017; in final form 13 September 2017)

Abstract—Ultrasound imaging is a commonly used modality for breast cancer detection and diagnosis. In this review, we summarize ultrasound imaging technologies and their clinical applications for the management of breast cancer patients. The technologies include ultrasound elastography, contrast-enhanced ultrasound, 3-D ultrasound, automatic breast ultrasound and computer-aided detection of breast ultrasound. We summarize the study results seen in the literature and discuss their future directions. We also provide a review of ultrasound-guided, breast biopsy and the fusion of ultrasound with other imaging modalities, especially magnetic resonance imaging (MRI). For comparison, we also discuss the diagnostic performance of mammography, MRI, positron emission tomography and computed tomography for breast cancer diagnosis at the end of this review. New ultrasound imaging techniques, ultrasound-guided biopsy and the fusion of ultrasound with other modalities provide important tools for the management of breast patients. (E-mail: bfei@emory.edu) © 2018 World Federation for Ultrasound in Medicine & Biology. All rights reserved.

Key Words: Breast cancer, Ultrasound imaging, Ultrasound-guided biopsy, Computer-aided detection, Image fusion, Three-dimensional (3D) ultrasound, Automated ultrasound, Detection and Diagnosis, Magnetic resonance imaging (MRI), Positron emission tomography (PET).

INTRODUCTION

Breast cancer is the most frequently diagnosed cancer and the leading cause of cancer death among females worldwide (Torre et al. 2015). Among women in the United States, breast cancer has the highest incidence of all cancers and is the second most common cause of cancer death after lung cancer (Siegel et al. 2015). It is estimated that there were 252,710 new cases of (30% in all cancers) and 40,610 deaths from (14% in all cancers) breast cancer in females of the United States in the year 2017 (Siegel et al. 2017). A woman living in the United States has a 12.3% or a 1-in-8 lifetime risk of being diagnosed with breast cancer (DeSantis et al. 2014). Early diagnosis is important for both treatment and the prognosis. Patients with smaller primary cancers at the time of their diagnosis have a significantly higher survival rate and a significantly reduced probability of dying from their cancer (Duncan and Kerr 1976). Early detection of breast cancer and accurate assessment of

lesions are the goals of various imaging modalities. As a conventional, medical imaging modality, ultrasound (US) has had a very important role in breast cancer detection, image-guided biopsy and lymph node diagnosis for many years.

We conducted the literature search within the PubMed database using the key words “Breast” and “Ultrasound” in the title field plus “Cancer” and “Ultrasound” in the Abstract/Title file for the period 1996 to 2017. We also used the Google Scholar database for an additional literature search. After reading the abstracts, we manually selected the relevant papers for this review. Each cited study had institutional review board/institutional animal care and use approval, which was part of the search criteria. In this review, we begin with an explanation of various ultrasound techniques, including ultrasound elastography, contrast-enhanced ultrasound, 3-D ultrasound, automatic breast volume scanning and computer-aided detection of breast cancer. We then provide an overview of ultrasound-guided breast biopsy and summarize ultrasound fusion with other imaging modality navigation systems. We also review the performance of various imaging modalities for breast

Address correspondence to: Baowei Fei, Department of Radiology and Imaging Sciences, Emory University School of Medicine, 1841 Clifton Road NE, Atlanta, GA 30329, USA. E-mail: bfei@emory.edu

lesion detection and lymph node diagnosis. Finally, we conclude with discussions and future directions.

ULTRASOUND IMAGING TECHNIQUES FOR BREAST CANCER DETECTION

Breast ultrasound imaging in the clinic

Ultrasound can assess the morphology, orientation, internal structure and margins of lesions from multiple planes with high resolution both in predominantly fatty breasts and in dense glandular structures. The general criteria for breast cancer detection with ultrasound are listed in [Table 1](#). Among those characteristics, surrounding tissue, shape, margin contour, lesion boundary and posterior acoustic features are significant factors to consider when classifying a lesion. Ultrasound has been used to classify benign, solid lesions with a negative predictive value of 99.5% ([Stavros et al. 1995](#)). The measurement results of tumor, including the “halo,” predict tumor size for invasive lobular carcinoma with high diagnostic accuracy ([Skaane and Skjorten 1999](#)). The Breast Imaging Reporting and Data System (BI-RADS) of the [American College of Radiology \(ACR 2015\)](#) has been widely used in most countries where breast cancer screening is implemented. BI-RADS is designed to reduce variability between radiologists when creating reports for mammography, ultrasonography or magnetic resonance imaging (MRI). The fourth version of the American Edition (2003) is completed by ultrasonography and MRI lexicons. As an extensive update of the Fourth Edition, the BI-RADS Fifth Edition (2013) made some revisions based on accumulated clinical practice. Observer variability of BI-RADS for breast ultrasound ([Lee et al. 2008](#)) indicates that inter- and intra-observer agreement with the BI-RADS Lexicon for US is satisfactory. The BI-RADS Lexicon can provide an accurate and consistent description and assessment of breast US. BI-RADS is integrated into the standard DICOM and is implemented directly on digital mammography stations and in computer-aided diagnosis (CAD) ([Balleyguier et al. 2007](#)).

Ultrasound elastography

Elasticity is a property of a substance. Deformation occurs when the body is subjected to external forces and the original shape or size is restored on removal of the external force. The slight deformation of tissue can be followed and marked by the speckle, ubiquitous and low attenuation of ultrasound images. Echo data are acquired by the high speed of ultrasound to observe tissue displacement ([Bamber et al. 2013](#)). Elastosonography has become a routine tool in ultrasonic diagnosis and measures the consistency or hardness of the tissues non-invasively to differentiate benign from malignant breast lesions.

Different categories for various elastographic techniques. Many different elastography techniques are available to measure and display elastography qualitatively or quantitatively, using the displayed modulus and different forces. Commonly used techniques are strain elastography (SE), acoustic radiation force impulse (ARFI) imaging, transient elastography (TE), point shear wave elastography (pSWE) and shear wave elastography (SWE). According to the property displays, there are three types: strain or strain rate, displacement and shear wave speed. Strain elastography calculates and displays tissue strain; ARFI imaging detects and displays tissue displacement; TE and pSWE record the shear wave propagation speed (without making an image); and SWE displays images of shear wave speed ([Bamber et al. 2013](#)). There are two types of applied forces in elastography: quasi-static, for example, by probe palpation; and dynamic, for example, by a thumping, vibrating, acoustic radiation force. Quasi-static force is induced mechanically, whereas dynamic force can be induced by ultrasound. SWE is quantitative, and its applied force is a dynamic force and needs to create shear. Other methods can use dynamic power, but can also use static or quasi-static force. Ultrasound-based elastography is created by a focused US impulse that transmits ultrasound pulses at a high speed from the same transducer without compressing the skin. ARFI imaging and SWE

Table 1. Characteristics of the sonogram evaluation of breast cancer

Lexicon	Malignant tumors	Benign tumors
Shape	Irregular	Oval, round
Orientation	Vertical, taller than wide, indifferent	Parallel, wider than tall
Margin	Indistinct	Circumscribed, identifiable, thin echogenic capsule
Margin contour	Irregular, angular, spiculate	Smooth, three or fewer gentle lobulations
Echogenicity	Markedly hypo-echoic	Hyper-echoic, iso-echoic or mildly hypo-echoic
Genicity	Homogeneous	Heterogeneous
Posterior features	Shadowing	Enhancement, no changes
Calcification	Microcalcification	Absent
Surrounding tissue	Architectural distortion	Compression, no alteration
Retraction phenomena	Present	Absent

Sources. [Chen et al. \(2013\)](#), [Gokhale \(2009\)](#).

are both based on an acoustic force created by the focused US impulse.

Strain elastography: Principle and applications. Strain elastography uses a hand-held probe with a slightly longitudinal pressing method or respiratory movement and obtains the hardness response information by estimating the deformation along the longitudinal axis and the strain distribution of the internal tissue. Strain elastography technology can be used to qualitatively and semiquantitatively study the elastic strain rate ratio of a lesion compared with that of the surrounding normal tissue. Compression technology is easy to implement, although it suffers from higher operator dependence and poor reproducibility. Real-time elastography (RTE), which generates “strain imaging” by compression, assesses the relative elasticity of the tissue in a specific area of interest, creating an elastogram, that is, a color-coded map, that is superimposed on the US image. The relative elasticity may vary according to the tissue studied, the size of the RTE box and the pressure exerted. As tissue is mechanically non-linear, the strain from a given force decreases with increasing force, and the tissue becomes harder as more force is applied. The resolution of strain image changes with different contrast discrimination of the strain and with window size or displacement, strain estimators and the smoothing window, palpation speed and amplitude, persistence, and so forth. There are some artifacts that may influence strain images, such as friction between the transducer and skin, which could decrease the strain of surface tissue; a narrow compressor, which generates limited strain with poor homogeneity and decays rapidly with depth; the artifact of strain concentration, which might be seen when there is a hard inclusion in a soft background and which can explain the high strain at slip boundaries and edge enhancement; and the “egg shell,” which might occur when soft regions are buried in a stiff

background, as stiff tissue prevents the generation of strain inside the egg. The features that help generate good strain images include closeness to the target and some distance to tissue boundaries, the anatomic plane and other structures.

An investigation of 169 *ex vivo* breast tissue samples (Samani et al. 2007) revealed that the elastic moduli of normal breast fat and fibroglandular tissue are similar, whereas fibroadenomas are approximately twice as stiff. Fibrocystic disease and malignant tumors exhibited a 3- to 6-fold increased stiffness, whereas high-grade, invasive ductal carcinoma exhibited up to a 13-fold increase in stiffness, compared with fibroglandular tissue (Samani et al. 2007). A 5-point scale was adopted according to the hardness of nodules in strain elastography (Itoh et al. 2006). Score 1 indicates deformability of the entire lesion; score 2 indicates deformability of most of the lesion with some small, stiff areas; score 3 indicates deformability of the peripheral portion of a lesion with stiff tissue in the center; score 4 indicates that the entire lesion is stiff; and score 5 indicates that the entire lesion and surrounding tissue are stiff. A lesion scoring from 1 to 3 points is considered benign (Fig. 1), whereas a lesion scoring 4 or 5 points is malignant. Among the 10 largest published studies using the 5-point scale and a cutoff value between 3 and 4 for assessing malignancy, Carlsen et al. (2013) compared the diagnostic performance of SE and B-mode US. All 8 studies had better sensitivity for B-mode than for SE, whereas 7 of these studies had better specificity and higher accuracy for SE than for B-mode imaging; combined B-mode and SE sensitivity decreased in 3 of 5 studies, whereas specificity and accuracy increased in 4 of 5 studies.

ARFI imaging. ARFI imaging employs a short acoustic impulse of high intensity to display displacement of tissue elements in a longitudinal direction and qualitatively creates a static map of the relative stiffness of the tissues

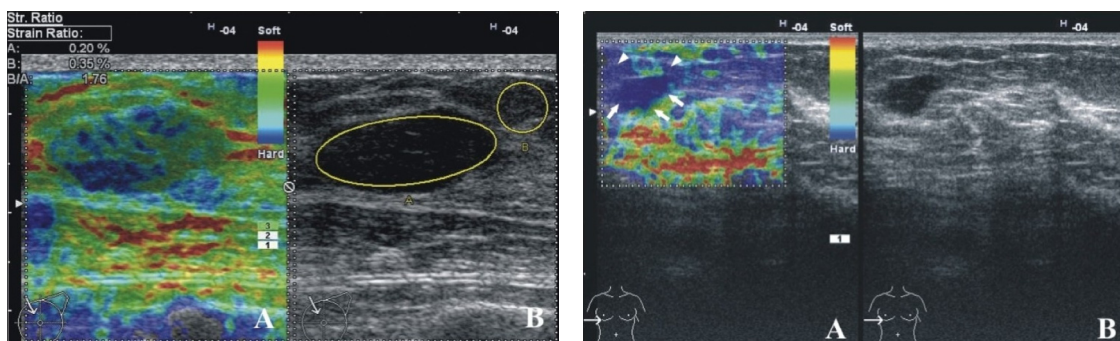


Fig. 1. Elastography could help to define biopsy location and characterize a complex lesion. Left: Strain elastography (SE) image (A) and B-mode ultrasonography (USG) image (B) reveal a hypo-echoic circumscribed lesion that is predominantly elastic and exhibits a mosaic pattern of green and blue. This was a fibroadenoma with a Tsukuba elasticity score of 2 and a strain ratio of 1.76. Right: SE image (A) and B-mode USG image (B). The lesion (arrows) and the surrounding tissue (arrowhead) were colored blue and had an elasticity score of 5. Pathology revealed an invasive ductal carcinoma. Reprinted from Gheonea et al. (2011).

within a small box. The tissue displacement can be accessed according to the area ratio (Li et al. 2015). Compared with strain elastography, ARFI imaging has better resolution, less inter-observer variability and less influence by the stress concentration and by slip movement anterior to the imaged region, and it exhibits a better image in deep tissue. However, the ARFI method can only create static images, not dynamic sequences such as strain images, and it also depends on absorption and reflection of the pushing beam and delay between the push and the displacement measurement. ARFI is not virtual tissue imaging (VTI). In the literature, pSWE has been described as ARFI quantification. pSWE has been used for shear wave speed measurement using radiation force excitation (Bamber et al. 2013). The quantitative method employs a primary acoustic impulse focused on a region of interest where it generates pressure waves in transverse propagation to deform the tissues. The primary impulse is followed by a few, interrogating impulses distributed in the surrounding tissues and designed to calculate the propagation velocity of pressure waves. The propagation velocity and attenuation of the waves are related to the stiffness and viscoelasticity of the tissue. The waves travel faster in stiff tissues than in non-stiff tissues. This quantitative method provides pressure-wave velocity, but no spatial distribution.

According to a meta-analysis (Li et al. 2015), ARFI elastography seems to be a good method for differentiating between benign and malignant breast lesions. The cutoff values for the shear wave velocity of VTQ ranged widely from 2.89 to 6.71 m/s, whereas the VTI area ratio only ranged from 1.37 to 1.66. Total sensitivity and specificity were 0.843 and 0.932 for the VTQ of ARFI and 0.864 and 0.882 for the VTI of ARFI, respectively (Li et al. 2015). According to other published studies, the mean VTI area ratio of the benign lesions, 1.08 ± 0.21 , differed from that of the malignant lesions, 1.99 ± 0.63 (Meng et al. 2011), whereas the mean shear wave velocity differed from 4.49 to 8.22 ± 1.27 m/s in malignant lesions and from 2.25 ± 0.59 to 3.25 ± 0.03 m/s in benign lesions (Bai et al. 2012; Meng et al. 2011; Tozaki et al. 2011).

SWE. Application of varying pressure to a tissue surface generates shear deformation, as well as longitudinal propagation. The propagation wave of shear deformation is used in sonography to obtain elastic information regarding tissue. SWE uses acoustic radiation force to obtain real-time 2-D or 3-D quantitative shear wave speed images. The speed of shear wave propagation is proportional to the Young's modulus (kilopascals, kPa), a measure of the resistance of tissue to shearing, which is currently used to quantitatively measure lesion elasticity (Athanasίου et al. 2010; Evans et al. 2010). The image is a semitransparent color overlap on a B-mode image in a region of interest and represents the distribution accord-

ing to the local propagation velocity of the pressure waves. Values of the maximum and average stiffness and the standard deviation can also be measured. SWE is quantitative and displays no stress concentration with less operator dependence. High pre-stress will cause a high SWE artifact in superficial tissue. The shear wave propagation near a boundary and thin layer might be invalid to assume the relationship between their speed and elastic modulus. As shear waves cannot propagate through pure fluid, SWE is sensitive to the average fluid content in tissue.

High mean stiffness values in SWE have been found to have a statistically significant positive association with the size of the invasion, high histologic grade, lymph node involvement, tumor type and vascular invasion for invasive breast cancer, which suggests that higher mean stiffness values indicate a poorer prognosis (Evans et al. 2012). The stiffness of malignant breast lesions may be influenced by the desmoplastic reaction of intra- and extranodular infiltration of interstitial tissue or infiltration of the intraductal component, except in medullary and mucinous carcinomas (Goddi et al. 2012). Berg et al. (2015) reported the median maximum stiffness (E_{\max}) on SWE of breast disease of various histopathologic grades (Fig. 2). SWE provides more information regarding unidentifiable breast lesions (Fig. 3). On SWE, Evans et al. (2012) reported that invasive tumors smaller than 10 mm had a mean stiffness of 64 ± 23 kPa (mean \pm standard deviation [SD]), that tumors between 10 and 20 mm had a stiffness of 129 ± 66 kPa and that tumors larger than 20 mm had a stiffness of 156 ± 45 kPa.

Clinical applications of ultrasound elastography. Some clinical questions are worth noting: (i) Pre-compression is the amount of pressure applied during scanning. Pre-compression can change the tissue's elastic properties in SWE. If sufficient pre-compression is applied, the elastographic properties of all tissues are similar (Barr 2012). With minimal pre-compression, the differences in shear wave speed for different tissues are maximized. Only a minimal amount of pre-compression is required to obtain a better-quality elastogram, whereas a moderate amount of pre-compression is needed to obtain better-quality B-mode images. (ii) Under some biological conditions shear waves cannot form an image; for example, if the shear wave velocity is too high it cannot be caught in extremely stiff cancer. When elasticity cannot be evaluated, the color display will turn off. This display should differ from that for a low shear wave elasticity of soft tissue areas. As cysts that are non-viscous liquid do not support shear waves, they appear black. (iii) The direction of a probe may affect shear wave velocity and should be considered in clinical applications. (iv) Shear wave propagation is depth limited. For lesions deeper than 4 cm, it may not be possible to obtain a result. Repositioning the patient to make the lesion closer to the

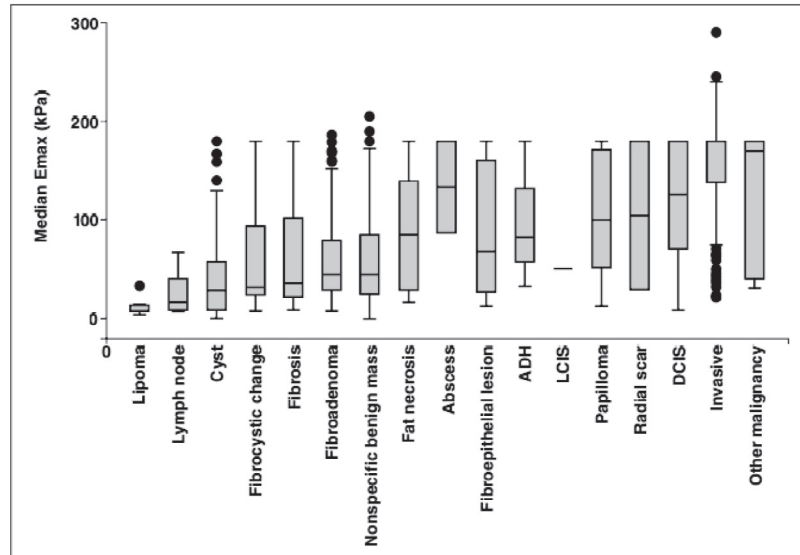


Fig. 2. Shear wave stiffness of breast masses. The box-and-whisker plot of the median maximum stiffness (E_{\max}) on shear wave elastography (horizontal lines in bars) as a function of the histopathologic diagnosis for 1562 sonographically visible breast masses. The boxes represent the interquartile ranges (IQRs [25th–75th percentiles]), and the whiskers represent the $1.5 \times$ IQR. Values outside whiskers are plotted as individual dots. ADH = atypical ductal hyperplasia; LCIS = lobular carcinoma *in situ*; DCIS = ductal carcinoma *in situ*. Reprinted from Berg et al. (2015).

skin surface can help in these cases (Barr 2012). (v) The size of a mass influences the SWF result, and it has been reported that smaller lesions have better sensitivity and specificity (Feng et al. 2010; Giuseppetti et al. 2005).

There has been controversy regarding the accuracy of breast ultrasound elastography compared with conventional B-mode ultrasound, and SWE was not significantly more sensitive than gray-scale ultrasound for the detection of either invasive ductal carcinoma or invasive lobular carcinoma (Sim et al. 2015). However, elastography can lead to a re-evaluation of the lesion (Fig. 4), and even lesions that appear echoic on B-mode imaging may have different strain properties. Four of 52 cases of lobular cancer were benign on both mammography and gray-scale ultrasound, but were suspicious on SWE (Sim et al. 2015). The diagnostic accuracy of SWE for solid breast lesions is at least as good as that of gray-scale ultrasound with BI-RADS classification (Evans et al. 2010). Elastasonography is a simple, fast and non-invasive diagnostic method that may improve the specificity (SP) of diagnostic breast cancer, especially for BI-RADS 3 (Scaperrotta et al. 2008). A prospective study in 939 patients proved that adding quantitative SWE features to the BI-RADS feature in adjustment 3 and 4a class breast masses could improve the specificity of breast US mass assessment without loss of sensitivity (Berg et al. 2012). Fausto et al. (2015) used the strain ratio, the ratio of glandular tissue to fat and the ratio of lesion to fat to improve diagnostic accuracy in BI-RADS 3 and 4 lesions (Fausto et al. 2015).

Elastography has been found to reduce the need for benign biopsies when they are used as a complementary tool to conventional ultrasound (Lee et al. 2013). Elastography could then help to define the location of a biopsy and characterize a complex lesion (Fig. 4). A recent study reported that anisotropy in 2-D SWE is an indicator of breast cancer (Skerl et al. 2016). A meta-analytic (Sadigh et al. 2012) comparison of the elasticity and B-mode revealed that elastography as a single test is not superior to B-mode alone, but that in low-risk patients it is recommended that elastography be performed after a positive B-mode result to decrease the rate of unnecessary biopsies.

Contrast-enhanced ultrasound

A tumor's vessel density is proportional to its size and pathological severity (del Cura et al. 2005). The high density of blood vessels and vascular distribution disorders are present in breast malignant lesions. To visualize vascular structures and tissues with different vascularity, contrast-enhanced ultrasonography (CEUS) is used in clinical research (Kim et al. 2003). CEUS uses intra-venously injected gas microbubbles to improve backscattering from the vasculature (Calliada et al. 1998). Microbubbles are specific gases encapsulated in various types of shells, with diameters between 1 and 7 μm ; are more echogenic than red blood cells; and are confined to intra-vascular spaces and do not leak through the vessel wall. SonoVue (Bracco, Milan, Italy), the commonly used contrast agent, is a blood-pool perfluoro gas agent that consists of microbubbles of sulfur hexafluoride (SF_6) stabilized by a phospholipid shell.

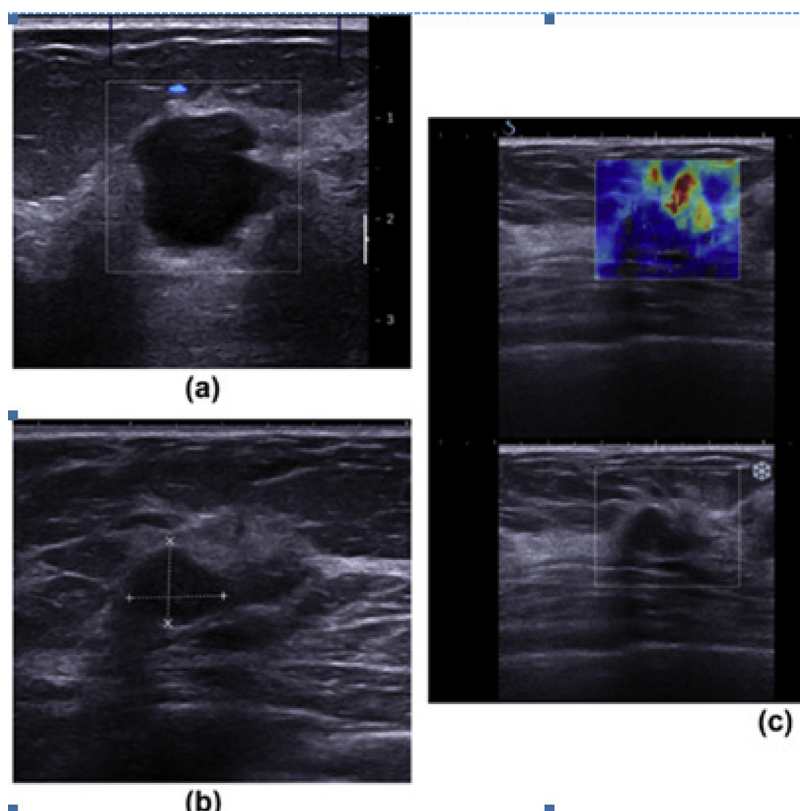


Fig. 3. Shear wave elastography in the diagnosis of invasive lobular breast cancer. A 47-y-old woman who had undergone a previous left mastectomy for ductal carcinoma *in situ* presented with a new lump in her right breast. (a) Ultrasound revealed benign cysts. (b) A well-defined, round lesion with posterior enhancement and mildly echogenic contents was thought to represent a thick cyst on gray-scale ultrasound, but (c) shear wave elastography increased stiffness at and around the lesion (mean elasticity of 147 kPa). Subsequent biopsy and surgery confirmed a grade 2 invasive lobular carcinoma. Reprinted from [Sim et al. \(2015\)](#).

Because of differences in the acoustic impedance and compressibility between the microbubbles and surrounding media, ultrasound contrast agents mainly act as non-linear scatters. Non-linear imaging techniques, including pulse inversion harmonic imaging, intermittent power Doppler and subharmonic imaging, are used to reduce bubble destruction and provide improved depiction of microvasculature. Combination of microbubble contrast agents with non-linear imaging techniques could reveal vascular morphology.

Contrast-enhanced ultrasound offers qualitative and quantitative analysis for characterizing breast lesions. After SonoVue administration, different perfusion phases can be identified, that is, early (0–1 min), middle (1–4 min) and late (4–6 min) phases ([Zhao et al. 2010](#)). CEUS-dedicated software produced the following parameters on time–intensity (TI) curves ([Figs. 5 and 6](#)): peak percentage; time to peak (TTP); mean transit time (MTT); regional blood volume (RBV); and regional blood flow (RBF). Enhancement patterns in the early phase and contrast medium persistence in the late phase differ in benign and malignant

breast lesions. The features of malignancy include early and fast enhancement in the early phase, centripetal filling, claw-shaped enhancement, higher maximum intensity and contrast medium accumulation in the late phase (see [Fig. 5](#)), whereas the features of benign tissue include delayed, centrifugal filling, homogeneous enhancement and seldomly contrast medium present in the late phase (see [Fig. 6](#)) ([Balleyguier et al. 2009](#); [del Cura et al. 2005](#); [Jung et al. 2005](#); [Zhao et al. 2010](#)).

Since 2011, the European Federation of Societies for Ultrasound in Medicine and Biology (EFSUMB) guidelines for CEUS of the breast remain an important topic for research, but have not been recommended for routine clinical use ([Piscaglia et al. 2012](#)). [Ricci et al. \(2007\)](#) found that the sensitivity and specificity of CEUS for differentiating malignant from benign breast lesions are 100% and 87.5%, respectively, and contrast-enhanced sonographic patterns correlated well with those provided by MRI. The positive predictive value (PPV) of CEUS evaluation was 91%, and the negative predictive value (NPV) was 73% ([Caproni et al. 2010](#)). The size of a

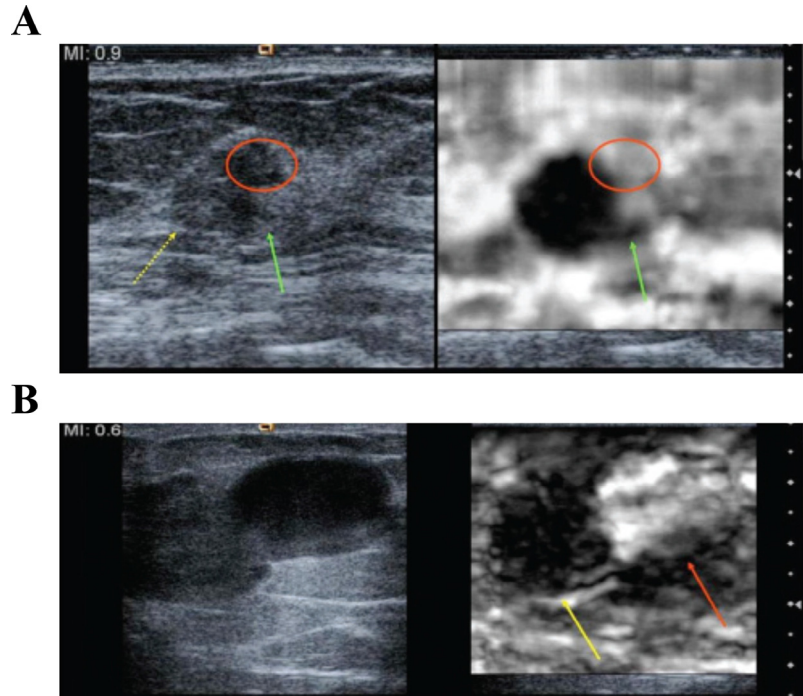


Fig. 4. Close evaluation of the elasticity patterns of a lesion can be helpful in their characterization and in biopsy planning. (A) Invasive ductal carcinoma with an area (red circle) that is “soft” on the elastogram. On pathologic examination from surgical resection, the soft area was a benign fibroadenoma and was not distinguishable from the invasive ductal carcinoma (yellow arrow) diagnosed in a 53-y-old patient from the B-mode image. A spicule (green arrow) of the tumor is better seen on the elastogram. (B) Images from an 85-y-old patient who presented with a bloody nipple discharge. On the B-mode image, there is a large, complex lesion. On the elastogram, it is possible to identify a hard component (yellow arrow) and a soft component (red arrow). On pathologic examination, the solid component was a papillary carcinoma and the soft area was old blood. Reprinted from Barr (2012).

breast lesion measured with CEUS is larger than that measured with conventional ultrasound. Pathologic examination of a mass with measurement discrepancy revealed primarily ductal carcinomas *in situ* (DCIS) (Fig. 7), invasive carcinoma with a DCIS component, adenoids with lobular hyperplasia in breast cancers and inflammatory cell infiltration in one granulomatous mastitis (Jiang *et al.* 2007). A mass with a well-defined margin has only a small possibility of having larger measurements on CEUS. Doppler ultrasonography with contrast agent injection is highly efficient and better for evaluating the response to neoadjuvant treatment and confirmation of tumor hypervascularized destruction before radiofrequency (RF) in local, recurrent breast cancer (Vallone *et al.* 2005) (Lamuraglia *et al.* 2005). Enhancement patterns and parameters of contrast-enhanced US may be useful in the non-invasive prediction of the prognostic factors of breast cancer (Wan *et al.* 2012).

3-D ultrasound

Three-dimensional ultrasound may offer new perspectives in the field of breast ultrasound. There are two

main types of 3-D ultrasound. One is the use of 2-D imaging equipment with a certain mechanical movement to reconstruct the 3-D ultrasound volume. The other is real-time volumetric echo, which uses a matrix array transducer that electronically scans a 3-D volume. Replacing a single row of elements in conventional linear transducers, the elements in a matrix array transducer are arranged in a 2-D grid. Matrix array generates a beam in both positions, thus forming an entire, pyramid-shaped volume (Kisslo *et al.* 2000). The probe is held still and patients are asked to stop breathing during the 1–3 s the ultrasound unit requires to generate the 3-D volume. Then three perpendicular reconstructed planar sections—sagittal, transverse and coronal planes—are displayed simultaneously on the ultrasound screen. The coronal reconstruction images can indicate the details of anatomy and spatial locations of a lesion and gland and, thus, potentially improve the characterization of breast lesions. A retraction phenomenon in the coronal plane of the 3-D volume is a special characteristic of breast cancer (Fig. 8). Three-dimensional ultrasound allows calculation of the corresponding volume. At the same time, in 3-D ultrasound the characteristics of the orientation,

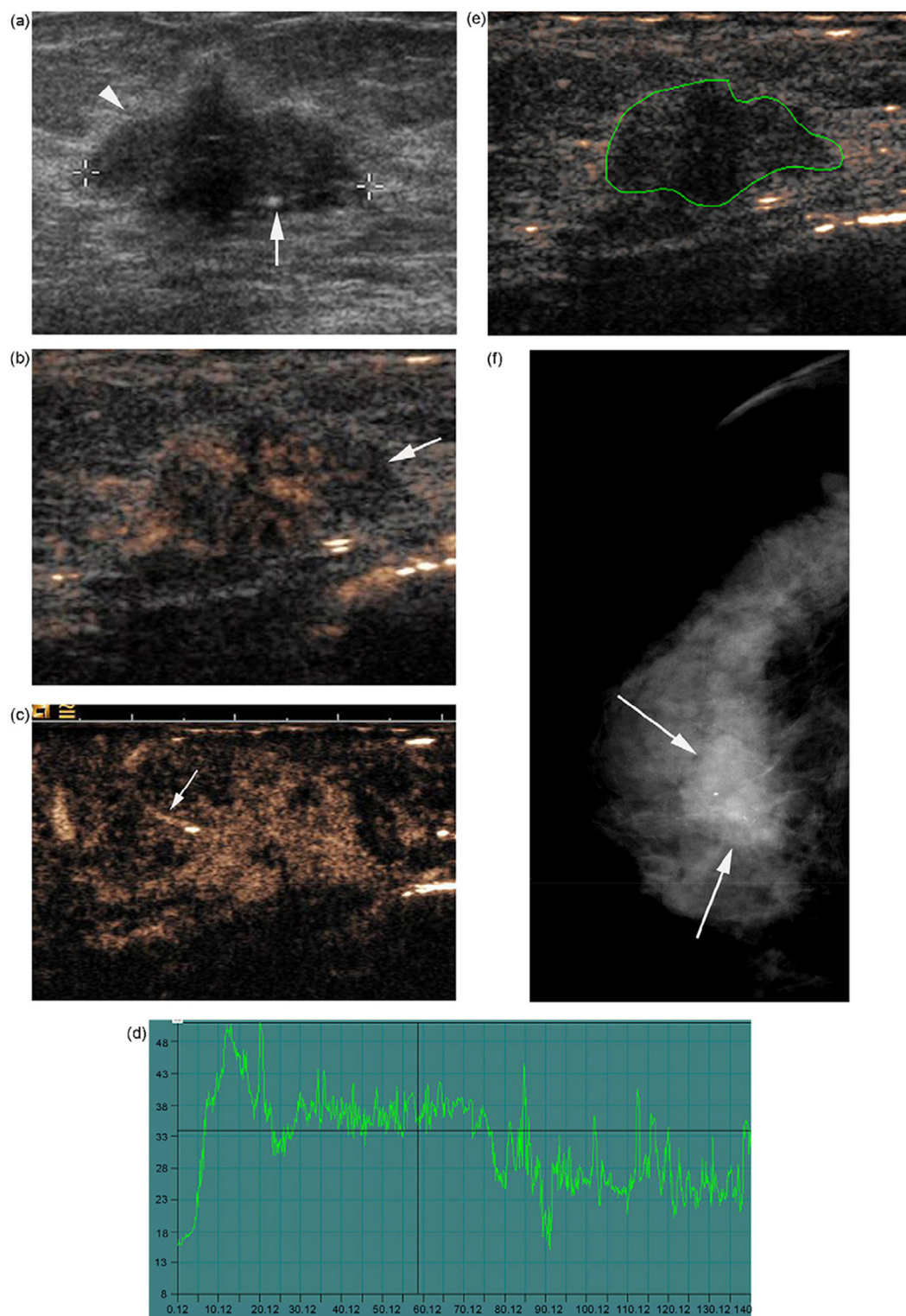


Fig. 5. Contrast ultrasound before and after contrast medium injection in a 66-y-old woman with 23-mm, ductal, infiltrative carcinoma. (a) B-Mode sonogram. (b) In the contrast mode (SonoVue) with coherence pulse sequencing and B-mode, the tumor is strongly enhanced after injection. Vessels are located in the peripheral area of the lesion. (c) In the contrast mode with coherence pulse sequencing only, the tumor-feeding artery is visible outside of the lesion (*arrows*). (d) Dynamic curve of enhancement after injection. Enhancement is fast; that is, the delay of peak enhancement was 10 s, and with a wash-out phase, the total time was 2 min. (e) Region of interest on the tumor to obtain enhancing curves. (f) Mammogram. Cranio-caudal view of the right breast. Reprinted from [Balleyguier et al. 2009](#)).

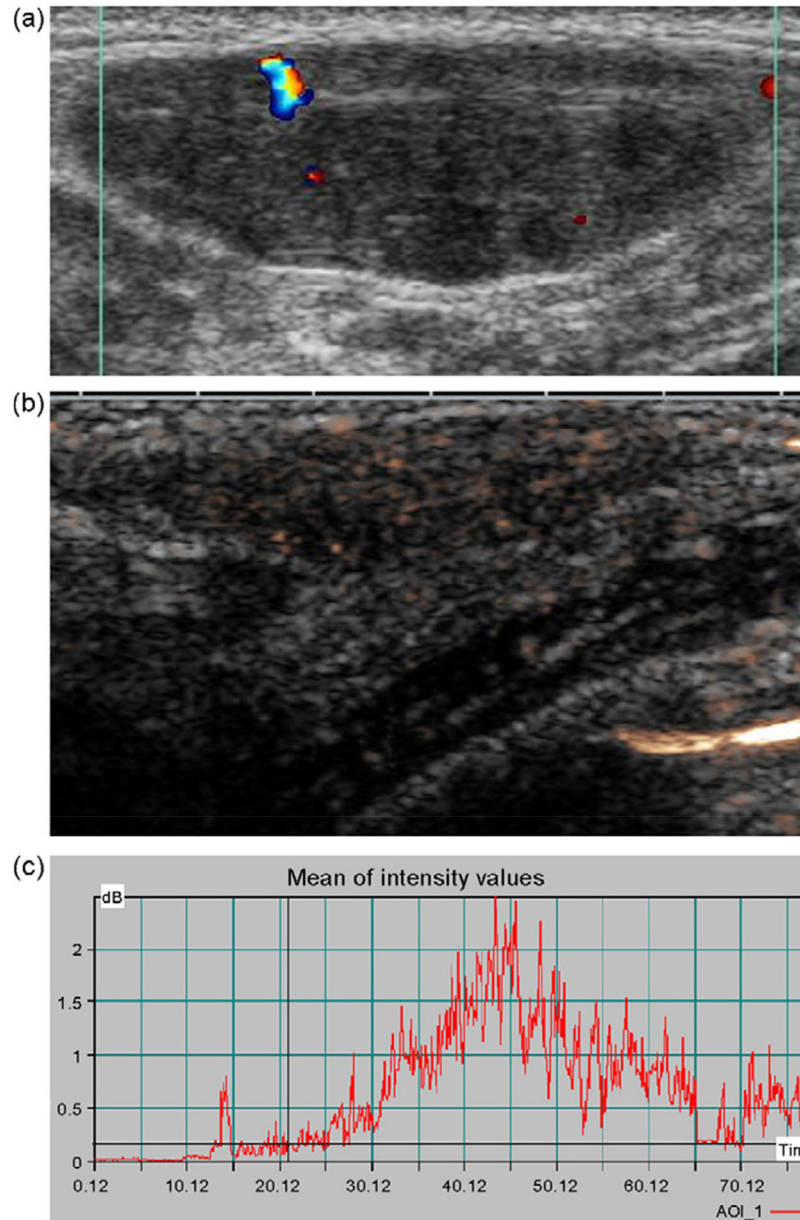


Fig. 6. Contrast-enhanced ultrasound of a 22-y-old woman with adenofibroma. (a) Color Doppler. Smooth contours, homogeneous content and posterior enhancement are criteria for benignity. (b) Contrast-enhanced ultrasound (SonoVue) with coherence pulse sequencing; thin and multiple arterial vessels are visible in the center of the lesion. Global enhancement is moderate and homogeneous. These enhancement parameters are suggestive of a benign lesion. (c) Enhancement curve. Enhancement is delayed compared with that of malignant tumors (>20 s). The enhancement value is also moderate compared with that of malignant carcinoma. The wash-out phase is longer. Reprinted from [Balleyguier et al. \(2009\)](#).

margin, margin contour and surrounding tissue in the conventional planes are still significant and independent parameters ([Watermann et al. 2005](#)).

A few preliminary studies have explored the use and advantages of 3-D CEUS in evaluating breast tumors ([Forsberg et al. 2004](#); [Jia et al. 2014](#); [Sridharan et al. 2015](#)). Forsberg compared the diagnostic ability for breast cancer evaluation of 3-D US with that of 2-D US and 3-D power

Doppler imaging and reported that the areas under the receiver operating characteristic curves of 2-D CEUS imaging are 0.51 and 0.76 for 3-D CEUS and, when 3-D CEUS is combined with mammography, 0.90 ([Forsberg et al. 2004](#)); The 3-D CEUS score for tumor angiogenesis agreed with that of contrast-enhanced magnetic resonance imaging (DCE-MRI) and correlated well with the biological factors, that is, microvessel density (MVD), vascular endothelial

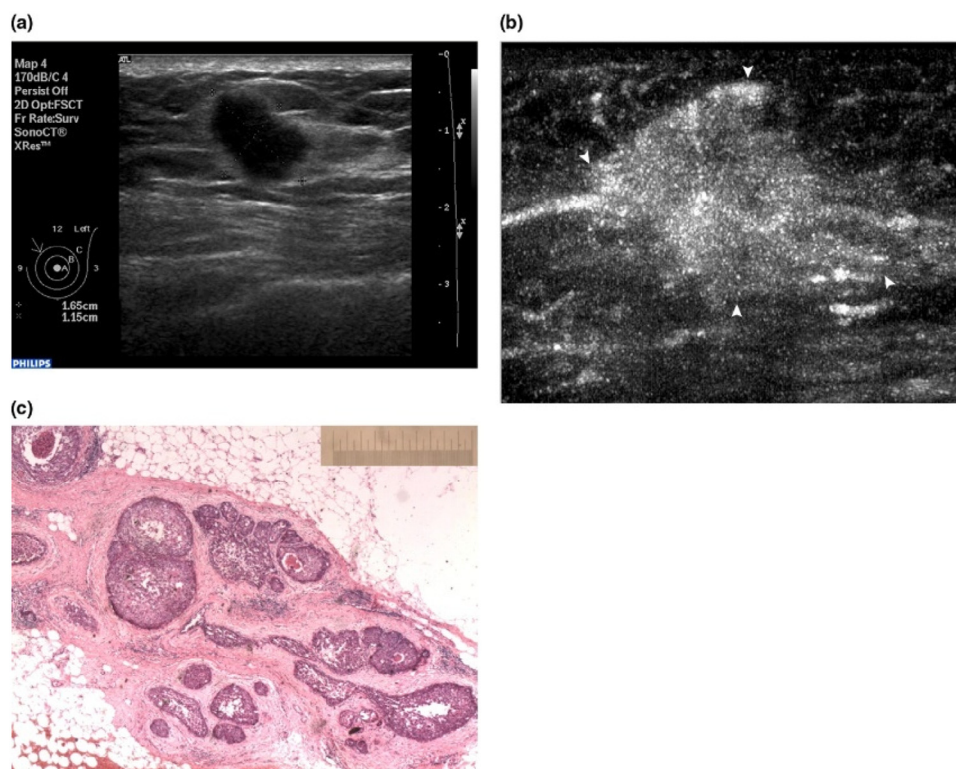


Fig. 7. Comparison of conventional ultrasound and contrast-enhanced ultrasound in a 47-y-old woman with a mass pathologically verified as low-grade ductal carcinoma *in situ*. (a) Conventional ultrasound: a 17×12 -mm mass surrounded by a hyper-echoic halo. (b) Magnetic resonance imaging: the mass exhibits diffuse enhancement (arrowhead) and increased in size to 22×16 mm. Large, enhancing blood vessels were not included in the measurement. (c) Photograph of the histopathological specimen (hematoxylin–eosin stain, original magnification $\times 20$): the difference in size corresponds to the extent of intra-ductal carcinoma. Reprinted from Jiang et al. (2007).

growth factor (VEGF) and matrix metalloproteinase (MMP-2, MMP-9) expression (Jia et al. 2014). Sridharan et al. (2015) reported that contrast-enhanced, 3-D subharmonic US could quantitatively evaluate the variations in vascular heterogeneity for benign and malignant breast lesions; that is, a benign lesion exhibits a significant difference in vascularity between the center and periphery, whereas in a malignant lesion there is no difference.

Automated breast sonography

Hand-held US (HHUS) is limited by operator dependence, non-reproducibility and its inability to image and store 3-D volumes of the breast. To overcome these limitations, an automated breast ultrasound system (ABUS) has been developed. This modality makes it possible to simultaneously visualize large sections of the breast from the skin surface to the chest wall and to store entire breast volumes on a picture archiving and communication system, thus enabling temporal comparison of current studies with relevant prior studies. In 2008, the SonoCine system received U.S. Food and Drug Administration (U.S. FDA) approval (Shin et al. 2015; U.S. FDA 2012). A standard US sensor can be mounted on an articulated arm and scans

the entire breast while the operator can adjust the angle and pressure of the transducer. The imaging produces the same image as 2-D hand scanning. This technique does not allow 3-D manipulation or reconstruction of the raw data. The imaging is reviewed in real time, as in any standard US examination, either at the time of the examination or later if the examination is recorded and stored. In September 2012, Somo-v ABUS systems were approved by the U.S. FDA for use in women with dense breasts who have negative X-ray mammography results and have not undergone previous, invasive procedures. With this system, a larger transducer paddle (Fig. 9) is placed over the breast and a small amount of compression is applied to stabilize the breast, scan and acquire the data (Shin et al. 2015). The US transducer might have to be repositioned to cover the entire breast. Three-dimensional data reconstruction is achieved by computer algorithms. As the process of ABUS is without change and is automatic, it does not require highly trained specialists and thus can eliminate technician fatigue. The acquisition time of ABUS is an average of 15 min for a patient with average-sized breasts (Shin et al. 2015). It takes a proficient radiologist 3–10 min to interpret a case of ABUS results, depending on the

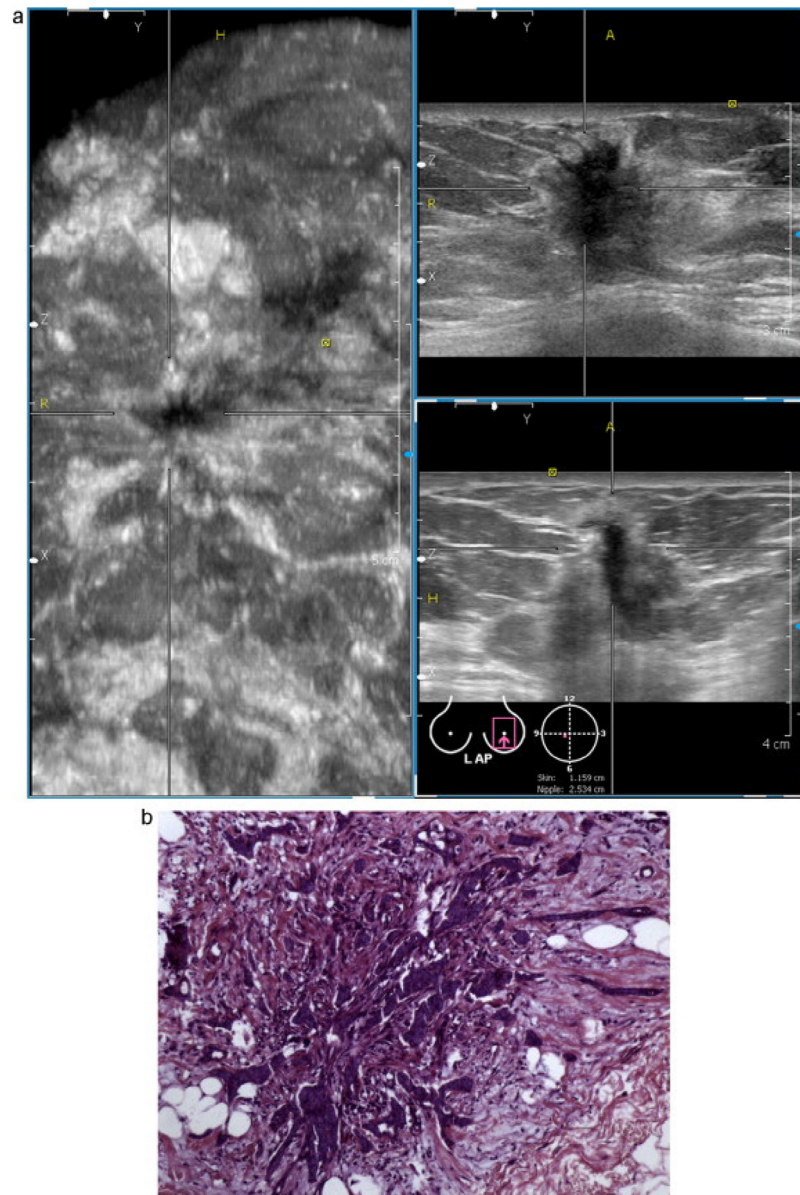


Fig. 8. (a) Automated breast volume scanning image of infiltrating ductal carcinoma. Note the heterogeneous echogenicity, spiculated border, indistinct margin and “taller-than-wide” appearance. (b) Histopathology image of the same mass. Note the infiltration of ill-defined glands into the surrounding collagenous stroma. Reprinted from Wang *et al.* (2012).

complexity (Kaplan 2014). According to the American College of Radiology Imaging Network (ACRIN) 6666 study, it takes a physician approximately 20 min for a full bilateral examination (O’Connell *et al.* 2013). Gel pad application for automated breast sonography is easy and provides significant pain relief, with the scan coverage expanded and the image quality maintained (Kim *et al.* 2015). Because of its digital capability, each sectional plane of the saved volume can be visualized (Fig. 10), thereby avoiding the investigator-dependent and non-standardized documentation.

Wenkel *et al.* (2008) reported that HHUS and ABUS are in good agreement ($\kappa = 0.83\text{--}0.87$) with the BI-RADS classification. In screening, the diagnostic quality of ABUS is similar to that of HHUS (Stoblen *et al.* 2011). The ABVS can provide more accurate information for assessing the extent and location of lesions than handheld US (Li *et al.* 2013; Shin *et al.* 2011). It could therefore improve the accuracy of detection of invasive cancers ≤ 1 cm (Kelly and Richwald 2011). Adding ABUS to mammography has improved callback rates, accuracy of breast cancer detection and confidence in callbacks for dense-breasted

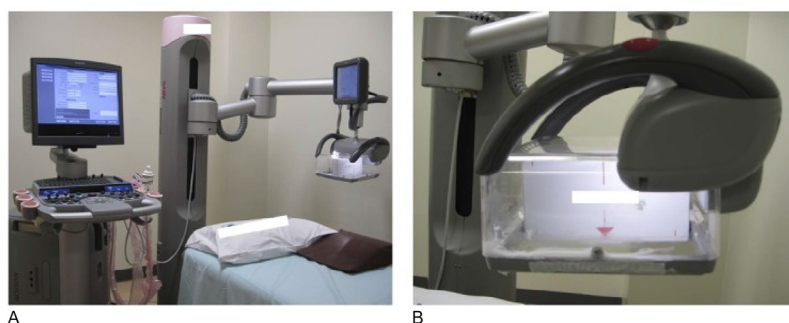


Fig. 9. Automated breast volume scanner. (A) Acuson S2000 ABVS (Siemens Medical Solutions). The transducer plate (B) is positioned over the breast and an automated scan is performed to obtain a series of 2-D images. Depending on breast size, more than three scans per breast may be required. Reprinted from [Shin et al. \(2015\)](#).

women ([Kelly et al. 2010](#)). The accuracy, SE and SP of ABUS for breast cancer diagnosis were 79.0%, 83.3% and 78.1%, respectively ([Wojcinski et al. 2013](#)). ABUS appears accurate in assessing the pre-operative extent of pure DCIS ([Li et al. 2013](#)). ABUS can reliably detect additional, suspicious lesions identified on breast MRI and may help in decisions regarding the biopsy guidance method, that is, US versus MRI, as a replacement tool for hand-held, second-look ultrasound ([Chae et al. 2013](#)). The large probe of ABUS provides the entire coverage and characterization of a large mass ([Fig. 11](#)), and it might provide an accurate measurement of a cancerous tumor >5 cm ([Shin et al. 2015](#)). ABUS can help to reveal intra-ductal abnormalities and the extent of these abnormalities in the ductal system ([Fig. 12](#)). Categorization of ultrasonographic findings using automated breast US is useful in predicting the likelihood of malignancy ([Tozaki and Fukuma 2012](#)). ABUS may have a role as a replacement tool for hand-held, second-look US ([Chae et al. 2013](#)).

Computer-aided detection for breast ultrasound

Breast ultrasound imaging and diagnosis are highly operator dependent and may have a high inter-observer variation rate. Moreover, with the large amount of data that needs to be analyzed when using automated 3-D breast ultrasound, the risk of oversight errors is substantial. Therefore, CAD is desirable to help radiologists in breast cancer detection and classification. CAD may be used as a second reader to improve radiologists' accuracy in distinguishing malignant from benign lesions on 2-D and 3-D US volumetric images.

A CAD system generally consists of four stages: pre-processing; segmentation; feature extraction; and selection and classification. Interested readers are referred to a more detailed review in [Cheng et al. \(2010\)](#).

Pre-processing. The main purpose of image pre-processing is to enhance the image and suppress speckle while preserving important diagnostic features. Speckle

noise reduction techniques generally involve filtering methods, wavelet domain methods and compound approaches ([Cheng et al. 2010](#)).

Segmentation. Image segmentation separates objects from the background and allocates regions of interest for feature extraction. The techniques include histogram thresholding, the active contour model, Markov random field and neural network. The active contour model combines prior knowledge regarding the relative smoothness of the 3-D mass shape, as seen on the US volumetric image, with information in the image data to decrease the interference of image speckles, posterior shadowing and variations of the gray level both within the mass and within the normal breast tissue. [Sahiner et al. \(2007\)](#) designed a computer algorithm to automatically delineate mass boundaries and extract features on the basis of segmented mass shapes and margins of 3-D US volumetric images.

Feature extraction and selection. After mass segmentation, the features are extracted from a malignant breast lesion and its margins for classification, including variance of intensities, entropy, average intensity, margin contrast, volumetric height-to-width ratio, sphericity, compactness, posterior acoustic behavior and speculation. These features can be divided into four categories: texture, morphologic, model-based and descriptor features. Most of these features are listed in BI-RADS. These features are also important for the design of CAD systems ([Moon et al. 2012](#)). Features extracted from each different section were combined to define case-based features for a given mass. The case-based feature vectors were fed into classifiers, such as linear discriminant analysis, with stepwise feature selection to obtain computer-estimated malignancy scores. It has been reported that texture features can distinguish malignant from benign lesions on 2-D US ([Gomez et al. 2012](#)). Another study ([Liu et al. 2014](#)) incorporated three important types of texture features, including local binary

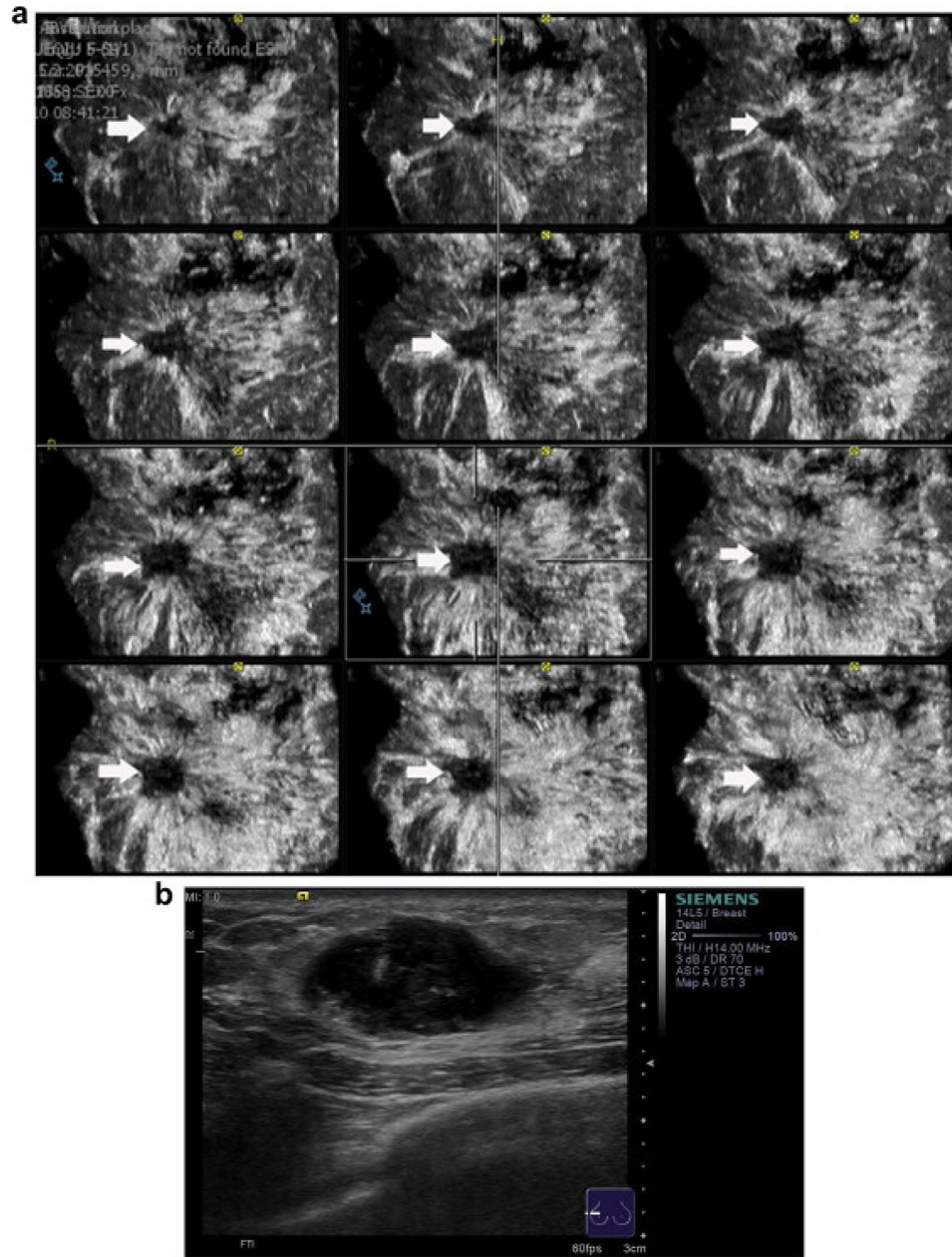


Fig. 10. (a) Automated breast volume scanner images of an invasive ductal carcinoma of the breast in a multislice view from the skin down to the thoracic wall in the coronal plane (the slices are 0.5 mm). (b) Handheld B-mode ultrasound. The typical retraction phenomenon of the mass is observed in several, consecutive coronal planes (*arrowhead* on the right). This indicates the conditions of the masses at different depths. Reprinted from [Chen et al. \(2013\)](#).

patterns (LBPs), gray-level co-occurrence matrix (GLCM)-based features and Gabor filters, to classify benign and malignant lesions in automated 3-D breast ultrasound images. LBP features from the area surrounding the segmented lesion, texture features of squares and autocorrelation and texture features based on 3-D GLCM could be used to classify the ABUS volumes of a breast lesion ([Liu et al. 2014](#)). The ranklet transform after texture features are extracted may be useful for improving the

ability to discriminate between triple-negative breast cancer and benign fibroadenomas ([Hipwell et al. 2016](#)). The phased, congruency-based binary pattern (PCBP) is an oriented local texture descriptor that combines the phase congruency (PC) approach with the LBP. [Tan et al. \(2015\)](#) used a large number of 2-D Haar-like features to differentiate lesion structures from false positives. [Chang et al. \(2015\)](#) used neutrosophic image transformation and fuzzy c-mean clusterings to define the lower and upper boundaries

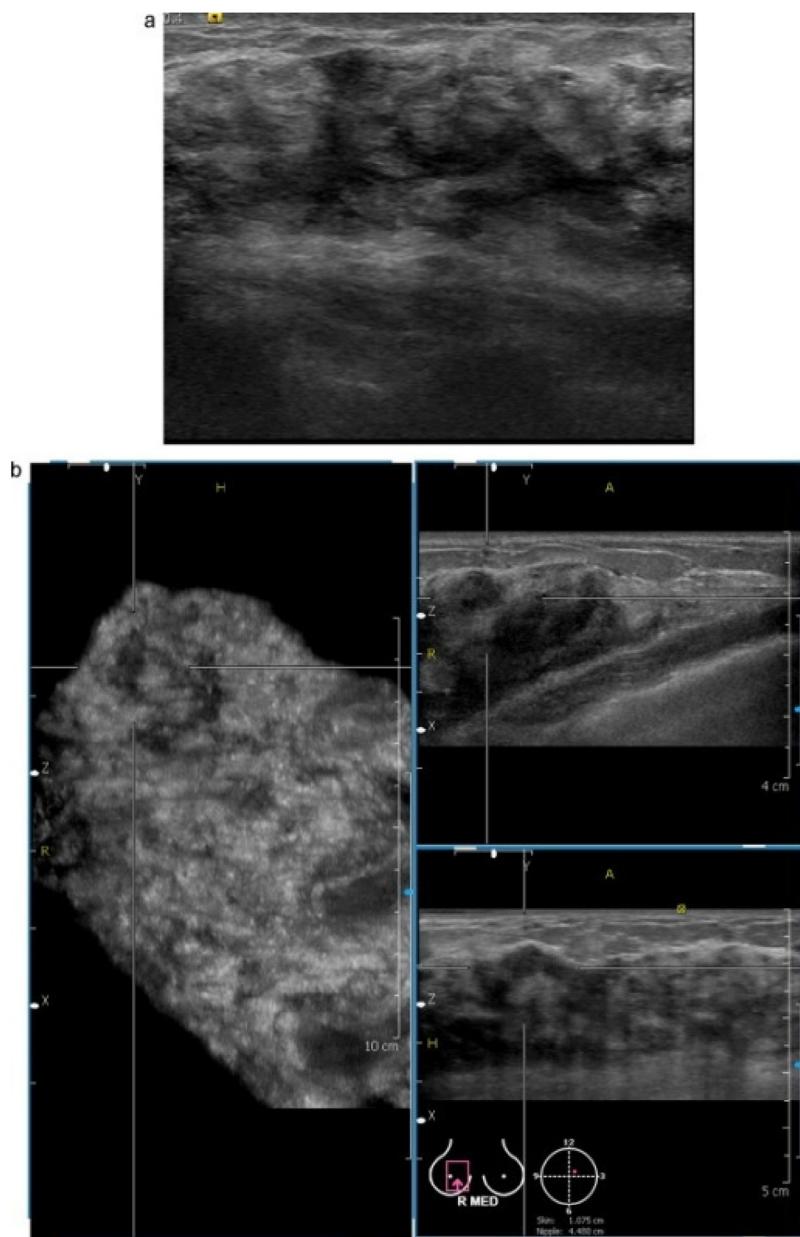


Fig. 11. Automated breast ultrasound of diffuse multiple invasive ductal carcinomas in a 29-y-old woman. (a) Hand-held ultrasound revealed a diffuse, hypo-echoic area in almost the entire right breast that was misinterpreted as adenosis. (b) Three-dimensional automatic breast volume scanner (ABVS) multiplanar images of the same area. This lesion was extensive (diameter = 6.5 cm), although the margin between the tumor and the surrounding normal parenchyma could be revealed with ABVS because of the wide scanning area. Reprinted from Wang et al. (2012).

of the fibroglandular tissue in US images and then extracted the number of hypo-echoic regions and histogram features. The detection result of the proposed system exhibited high agreement with results of the radiologists.

Classification. The selected features were fed into a classifier to categorize the images into lesion/no lesion or benign/malignant classes (Cheng et al. 2010). The commonly used classifiers include linear classifiers, artificial

neural networks, Bayesian neural networks, decision tree, support vector machine and template matching. Nagarajan et al. (2013) proposed a method to classify mass regions by building an ensemble classifier that employs Gabor features and achieved the best result. Support vector machines (SVMs), which use a structure risk minimization to diminish the error of the learning machine, have been widely used for tumor classification (Cai et al. 2015). Use of a cascade of Gentle Boost classifier that combines these

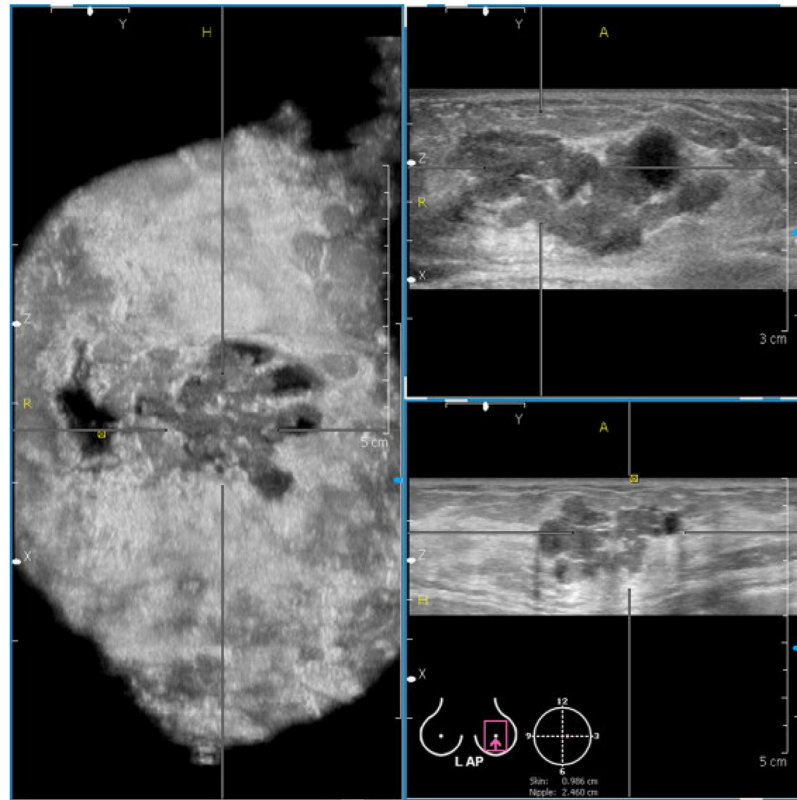


Fig. 12. Automated breast ultrasound of an 11-y-old girl with a palpable mass (intra-ductal papilloma) in the left breast. These scans revealed three orthogonal planes of the anterior–posterior left breast, that is, coronal reconstruction (left image), axial original plane (upper right image) and sagittal reconstruction (lower right image). In the coronal plane, dilated lactiferous ducts can be detected, as can intra-luminal echoes. Reprinted from Wang *et al.* (2012).

features can improve their previously developed CAD system in the initial candidate detection stage. A machine learning methodology in which adaptive boosting is paired with selective pruning achieved high diagnostic performance without the added cost of an additional reader for differentiating solid breast masses by ultrasound (Venkatesh *et al.* 2015). A leave-one-case-out resampling method was used to train the classification system and to obtain the malignancy scores (Sahiner *et al.* 2007), and this method improved the radiologists' accuracy in distinguishing malignant from benign breast masses on 3-D US volumetric images. Bhatti *et al.* (2001) used speed-weighted pixel density to quantify vascularity in and around each mass and concluded that combining the vascularity measure with age can improve the discrimination of sonographically detected breast masses.

A CAD system can help readers to assess the probability that a particular lesion is malignant. The average area under the receiver operating characteristic curve for radiologists using CAD to discriminate malignant masses from benign masses on 3-D volumetric US images was increased from 0.83 (range: 0.81–0.87) to 0.90 (range: 0.86–0.93) (Sahiner *et al.* 2007). The CAD system improves the

performance of less experienced readers in distinguishing malignant from benign lesions in ABUS (Tan *et al.* 2013).

Summary and future directions

Breast cancer detection is a widely used application of ultrasound imaging in the clinic. Ultrasound elastography and contrast-enhanced ultrasound provide additional information on breast lesions based on duplex sonography. Elastography imaging is a qualitative and quantitative technique involving tissue stiffness or hardness rather than anatomy. However, elastography images cannot distinguish between lesions and surrounding tissue when their elasticity properties are the same. The quality of the elastography image is limited by the depth of a lesion. Combination of B-mode and elastography could overcome these problems. Uniform standards for elastography commercial systems and uniform clear classification for elastography commercial modes are needed. A convenient system for elastography information could make elastography more widely used in clinical practice with respect to breast disease. Contrast-enhanced ultrasound displays the vascular structure and perfusion of breast tumors

and provides quantitative parameters on the time–intensity curve, which are useful for discriminating between benign and malignant lesions and follow-up after local treatment. Automated breast US provides useful information regarding breast lesions, from their coronal reconstruction plane and the extensive field of transverse and sagittal planes, with the advantage of consistent acquisition images, time savings and less fatigue of the operator. In the next section, we continue to discuss the use of ultrasound for image-guided biopsy of breast cancer.

ULTRASOUND IMAGE-GUIDED BIOPSY OF BREAST CANCER

Various biopsy methods for the breast

Image-guided breast biopsy is currently the gold standard for the pathologic evaluation of breast cancer. It can be performed safely and reliably with minimal invasiveness in clinical practice and with increased patient convenience and decreased cost (Roe et al. 1997). Ultrasound, stereotactic mammography, MRI and positron emission mammography (PEM) are now successfully used to guide the biopsy needle to obtain a proper tissue sample that can be histologically assessed. The choice of image guidance for biopsy is based on a variety of factors, including which modality best visualizes the lesion, the physician's clinical experience, patient comfort, cost, ease of access and equipment availability. The common methods of biopsy include fine-needle aspiration biopsy, vacuum-assisted biopsy and core-needle biopsy. Meta-analysis of the various diagnostic biopsy methods for women at average risk of cancer revealed that SE estimates were higher than 0.90 and SP estimates were higher than 0.91 for all methods (Dahabreh et al. 2014).

Fine-needle aspiration biopsy (FNAB) of the breast has been considered a reliable sampling and less invasive morphologic diagnostic method. This method reduces health care costs and the psychological pressure for the patients. FNAB can be performed freehand for breast lesions that are palpable; for non-palpable breast lesions, it can be guided by ultrasound or mammography. Cytopathology for small-sized samples obtained by fine-needle aspiration provides the necessary information, although it does not assess tissue architecture. In a prospective study involving palpable nodules with a diameter >2 cm, fine-needle aspiration cytology had an SE of 90.4% and core biopsy had an SE of 95.2% (Dennison et al. 2003). In a blinded analysis, the SE of FNAB cytology was 92% and the SP was 83% (Reinikainen et al. 1999). However, FNAB has the drawback of inadequate or non-diagnostic cytologic samples and a high false-negative rate (Delle Chiaie and Terinde 2004).

Core-needle biopsy can be performed with an automated core-biopsy gun or a hand-held biopsy needle.

Automated core needles come in different sizes, that is, 14, 16 and 18 gauge. The quantity and quality of breast biopsy specimens depend on the needle size. Among the three needle sizes, 14-gauge, long-throw biopsy needles may provide the highest-quality core samples for breast biopsy (Helbich et al. 1998). The samples are sent for histologic examination, which is considered to be more reliable than fine-needle aspiration. Because core-needle biopsy samples only part of the breast abnormality, it seems to have a lower risk of complications than open surgical biopsy. The incidence of severe complications with core needle biopsy was less than 1%. The adverse events include hematomas, bleeding, vasovagal reactions and infections. The proportion of patients experiencing any of these adverse events was less than 1.5% (Dahabreh et al. 2014). There are potential risks of displacement of cancerous cells during biopsy; however, the clinical significance of these findings is unclear and tumor development on the biopsy-needle track is extremely rare.

Vacuum-assisted biopsy (VAB) was performed with an 11- or 10-G needle (Mammotome or EnCore or other Breast Biopsy System). In the review of the Brown Evidence-Based Practice Center, vacuum-assisted biopsy is also included with core-needle biopsy (Dahabreh et al. 2014). Once the needle is inserted and rotated in the sampling chamber, tissue samples are captured from different areas of the lesion that are double the size of those obtained by conventional core needle biopsy. It can be used to remove a small, benign lesion and decrease the underestimation of atypical ductal hyperplasia (ADH) and DCIS (Burbank 1997). The core biopsy and VAB system are usually guided by stereotactic mammography or ultrasound. The differences in SE and SP between US-guided automated and vacuum-assisted biopsy are 0.01 and –0.01 (Dahabreh et al. 2014).

Ultrasound- and stereotactic mammography-guided biopsy

Ultrasound-guided biopsy is easy to perform and radiation free. Operators can observe the plane and the angle between the lesion and the needle in real time and verify and flexibly adjust the direction of the needle position (Lieberman et al. 1998; Parker et al. 1993). A new needle guidance system was developed that couples the transducer with three, rotational joints to eliminate the need to align the ultrasound scanning plane with the needle and displays the needle trajectory before the insertion so that the participant can focus solely on the guidance of the needle toward the intended target lesion (Bluvol et al. 2009). Sometimes 2-D ultrasound is misleading with the artifactual appearance of the correct needle placement when it is positioned at the edge of a lesion. This inaccurate information can be compensated for with 3-D ultrasound. The advantages of 3-D ultrasound validation include a

reduction in the number of core samples required to achieve a reliable histologic diagnosis and a possible reduction in the risk of tumor cell displacement (Delle Chiaie and Terinde 2004; Smith *et al.* 2001). A retrospective study reported that the false-negative rate of US-guided 14-gauge CNBs for breast lesions rate was 2.0% with a sensitivity of 95.4% (Jung *et al.* 2017a, 2017b).

Stereotactic mammographic biopsy accounts for nearly half of all image-guided biopsies. Stereotactic mammographic biopsy is suitable for microcalcifications, distortions and focal densities, but it is limited by weight and breast thickness restrictions. Keranen *et al.* (2016) reported that the accuracy and clinical usefulness of vacuum-assisted biopsy using US guidance for breast microcalcifications was comparable to those of stereotactic guidance. Radiologic stereotactic mammograms and sonograms can also be used for pre-operative localization by wire. Percutaneous biopsy of a non-palpable breast mass using either US or stereotactic guidance is less expensive than surgery, and the cost savings are greater with US-guided biopsy (Lieberman *et al.* 1998).

Summary and future directions

Image-guided biopsy is another important application of ultrasound techniques in addition to detection of breast cancers. Ultrasound-guided biopsy is a pathway to pathologic diagnosis and treatment selection. Because different imaging techniques may have complementary roles, combination of ultrasound with different imaging modalities could further improve biopsy accuracy in the future. In the next section, we discuss the combination of ultrasound with MRI, PET, CT and mammography for breast cancer diagnosis and biopsy.

COMBINATION OF ULTRASOUND WITH MRI, PET, CT OR MAMMOGRAPHY

Ultrasound–MRI fusion-guided diagnosis

Because of the high SE (Harms *et al.* 1993) of breast MRI and the flexibility of US, research regarding the integration of sensitive MRI and real-time ultrasound has been conducted for many years (Curiel *et al.* 2007). In 2000, it was reported (Obdeijn *et al.* 2000) that the combined approach of MR imaging, sonography and aspiration fine-needle cytology is a good alternative to MR imaging-guided biopsy for revealing unknown primary sites in women with axillary lymph node metastases from adenocarcinoma. In this section, we discuss ultrasound fusion with MRI diagnosis for breast cancer, including second-look ultrasound and ultrasound combined with supine–MRI fusing volume navigation technique.

Second-look ultrasound. Second-look US (SLUS) is an additional, targeted breast imaging examination in which the lesions found on MR images can be located by SLUS

and can be histologically clarified by US-guided biopsy. The term *second look* is used even when there is no initial US examination. Regardless of whether antecedent, bilateral, whole-breast US is performed, SLUS is usually recommended before MR imaging-guided biopsy. Spick and Baltzer's (2014) study indicated the variable utility of SLUS in MR imaging-detected lesions and found that 57% (22.6%–82.1%) of MRI lesions can be located by SLUS and can be histologically clarified by US-guided biopsy (Spick and Baltzer 2014). SLUS more frequently detected foci (67%) and masses (73%) than it did non-mass-like lesions (54%). Rim enhancement in masses and clumped enhancement in non-mass lesions were also significantly more likely to have an ultrasound correlate (Meissnitzer *et al.* 2009). The detection rate of SLUS was independent of the lesion size on MRI, and malignant lesions were less likely to be detected on SLUS than benign lesions (Candelaria and Fornage 2011).

Park *et al.* (2013) summarized how second-look ultrasound can detect breast lesions with a suspicious MRI appearance. First, it is required that the location of each lesion on US be based on axial MR images that show the lesion's location relative to the mammary zones. Because 73% of mammographically detected cancers developed in a 1-cm-wide zone beneath the subcutaneous fat or anterior to the retromammary fat (Stacey-Clear *et al.* 1993), on second-look sonography the operator should pay significant attention to areas surrounding the mammary fascia (Nakano *et al.* 2012a, 2012b). Second, the lesion's location must be estimated according to the lesion-to-nipple distance. Third, surrounding tissues should be taken into considerations during the examination. The anterior and posterior mammary fascias and the adjacent tissue are important factors in correlating lesions on breast US. Fourth, based on lesion size, shape and other characteristics are used to locate the lesion. As lesions are compressed in a vertical direction by the US probe, they tend to appear smaller, and round lesions tend to appear oval or elliptical compared with their appearance on MR images. Furthermore, co-existing lesions, including ductal extension, known fibroadenomas, cysts, scars, implants or a known index cancer are good landmarks to differentiate between MRI and US.

Rationale of MRI image fusion with US-guided biopsy. Although SLUS enhancements in 70% (128/182) of unsuspected abnormalities were found on breast MRI, there were still 30% (54/182) that were sonographically occult, including 15% (8/54) cancer (Destounis *et al.* 2009). It is widely accepted that MRI-guided biopsy is very useful (Griebsch *et al.* 2006; Harms *et al.* 1993; Kuhl *et al.* 2000; Leach *et al.* 2005; Nunes *et al.* 1997; Weinreb and Newstead 1995). Results of MRI-guided methods for women at an average risk of cancer

revealed an SE and SP of 0.9 (0.57–0.99) and 0.99 (0.91–1.0) for automated biopsy and 1.0 (0.98–1.0) and 0.91 (0.54–0.99) for vacuum-assisted biopsy, respectively, and for women at a high age risk of cancer, the SE and SP are 0.90 (0.58–0.98) and 0.99 (0.92–1.0) for automated biopsy and 0.99 (0.98–1.0) and 0.92 (0.61–0.99) for vacuum-assisted biopsy, respectively (Dahabreh et al. 2014). Sakamoto et al. (2010) considered that the higher false-negative rate of US-VAB for MRI-detected lesions (26%) than for US detected lesions (7.4%) was caused by the difficulties in MRI–US correlation and indicated the need for MRI-guided biopsy.

Magnetic resonance imaging-guided biopsy is time and cost consuming, and the prone patient position increases their inconvenience and tension. For MRI-guided biopsy, a patient in the prone position is repeatedly transferred in and out of the unit to estimate the location of the lesion and confirm placement of the needle. As the lesion might move during needle insertion, and the position of the biopsy needle cannot be displayed in real-time images, there might be an error in sampling. Several robotic systems and actuators for MRI-guided applications are being developed. US-Guided biopsy has considerable advantages over MR imaging-guided biopsy, including its accessibility, efficacy, real-time visualization of lesions and biopsied tissue, cost-effectiveness and decreased stress and discomfort for the patient. Therefore, it is necessary to construct a system combining MRI imaging and a sonogram.

Combined real-time MR and US ultrasound navigation system (RtMR-US)

With real-time volume navigation development, US examinations and US-guided biopsies can be navigated using other imaging data. The structures invisible to US but visible to other imaging modalities can be operated using US-guided biopsy navigated by the other modality. The number of identifiable lesions seen on US and the accuracy of image-guided intervention are increased if co-registration is performed.

Technique and principle. Because information regarding fusion medical imaging was obtained using different imaging modalities, spatial registration is required to ensure that each pixel from different data sets represents approximately the same volume. Hipwell et al. (2016) reviewed the current research and relevant publications on breast biomechanics modeling, breast image registration and simulation algorithms. Image registration and data redistribution require manually co-registering a series of key points based on anatomic structures and the location of a lesion or fiducial markers before computer processing. The registration algorithm requires the measurement and identification of the orientation of the

coordinate's marker and transformation matrix to ensure that the same point is marked on each image. The image fusion could be maintained in stasis and real time. In static fusion, the 3-D image data of two modalities are stored in one workstation; after the data of two modalities are co-registered, the structure and lesion of each modality can be easily compared and evaluated on the fusion image. In real-time fusion, MRI/PET/CT data are saved in the US-guided navigation systems, and the MRI/PET/CT image of the aligned plane is displayed in real time during an ultrasound examination and intervention. Patient movement and the difference in between examinations can lead to distortion and affect the entire image fusion. Real-time fusion of ultrasound with MRI or CT is commercially available in brain, breast, liver, prostate, kidney, musculoskeletal, endoscopic ultrasound and interventional modalities (Ewertsen et al. 2013).

The real-time MR and US ultrasound navigation system (RtMR-US) navigation system enables simultaneous display of the same site by both imaging modalities side-by-side or superimposed. Breast MRI should be performed with the patient in the same position as on ultrasound, that is, the supine position with the arm raised. As a skin marker, before MRI, three vitamin E soft-gel capsules can be fixed at 3, 9 and 12 o'clock on the nipple (Pons et al. 2014). After MRI, the skin markers are covered with a transparent dressing to replace the soft gel capsules. The MRI data in the format of digital imaging and communications in medicine (DICOM) are transferred to the ultrasound-guided, virtual navigation systems. The small sensor installed in the ultrasonic probe and electromagnetic tracking system, that is, the electromagnetic transmitter, provides information regarding the position and orientation for the fusion system. Figure 13 illustrates the US and RtMR-US systems. The rigid transformation matrix allows probe movement and makes rotations arbitrary. As the patient is being scanned using sonography, the navigation system identifies the position and motion of the probe and simultaneously reconstructs a corresponding slice of MRI from the previously imported volume data. The MRI of multiplanar reconstruction corresponding to the sonography image displayed real time at a rate exceeding 10 frames/s (Nakano et al. 2009). When movement disturbs the co-registration image, adjusted function could be used for resynchronization.

Clinical research and results. A few studies have been published regarding the clinical applications of the ultrasound-MRI-guided system for breast biopsy. Preliminary experience by Fausto and co-workers (Fausto et al. 2012) indicated that the volume navigation technique of combined US-MR of the breast in normal breast tissue appears to be feasible, accurate and reproducible. Live US images combined with contrast-enhanced MR are able to

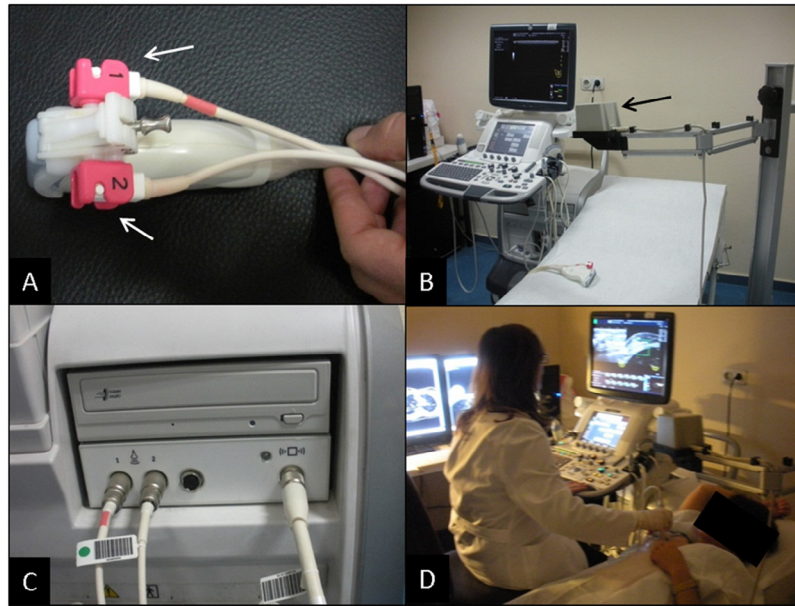


Fig. 13. Ultrasound and the real-time magnetic resonance and ultrasound navigation system (RtMR-US) system. (a) Electro-magnetic sensors on the tip of the probe (*white arrows*). (b) Electromagnetic transmitter (*black arrow*). (c) Connection unit between the lector magnetic transmitter, sensors and navigation system. (d) RtMR-US examination after co-registration. Reprinted from [Pons et al. \(2014\)](#).

reveal the morphology of the glandular tissue with specific anatomic details ([Fig. 14](#)). [Pons et al. \(2014\)](#) studied the diagnostic performance of RtMR-US for breast lesions and axillary lymph nodes found on MRI and not on second-look US. The detection rate of the navigation technique (90.7%) was higher than that of conventional US (43%). The diagnostic performance of the MR-US navigation technique for identifying malignant nodules among overall lesions and axillary lymph nodes had sensitivities of 96.3% and 100%; specificities of 18.8% and 30.7%; positive predictive values of 66.7% and 43.7%; and negative predictive

values of 75% and 100%. [Nakano et al. \(2009\)](#) conducted a series of studies using real-time virtual sonography (RVS) to detect breast cancer. They reported the sensitivity of RVS combined with MRI to be 98% for breast tumors and 83% for incidentally enhancing lesions. [Nakano et al. \(2012a, 2012b\)](#) found that 90% of MRI-detected lesions were identified with second-look sonography using RVS, whereas the rate of detection of MRI-detected lesions using conventional B-mode was limited to 30%. In their research of 2012, they found that RVS combined with MRI can identify many more occult lesions than conventional B-mode,

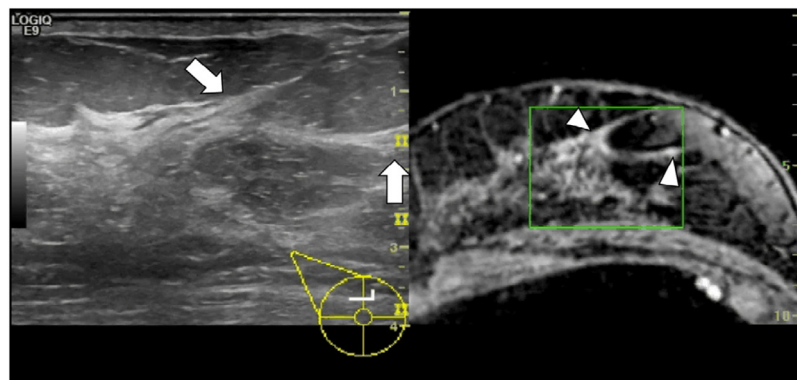


Fig. 14. Glandular tissue and a Cooper's ligament are shown at the confluence of the upper quadrant of the right breast. Live ultrasound (*white arrow*) using the volume navigation technique and using a late phase of contrast-enhanced magnetic resonance (*white arrowhead*) are both able to image the morphology with sharp anatomic detail. Because of the smaller magnification of the magnetic resonance image, a *green box* is electronically displayed on the magnetic resonance image, indicating the ultrasound scan area. Reprinted from [Fausto et al. \(2012\)](#).

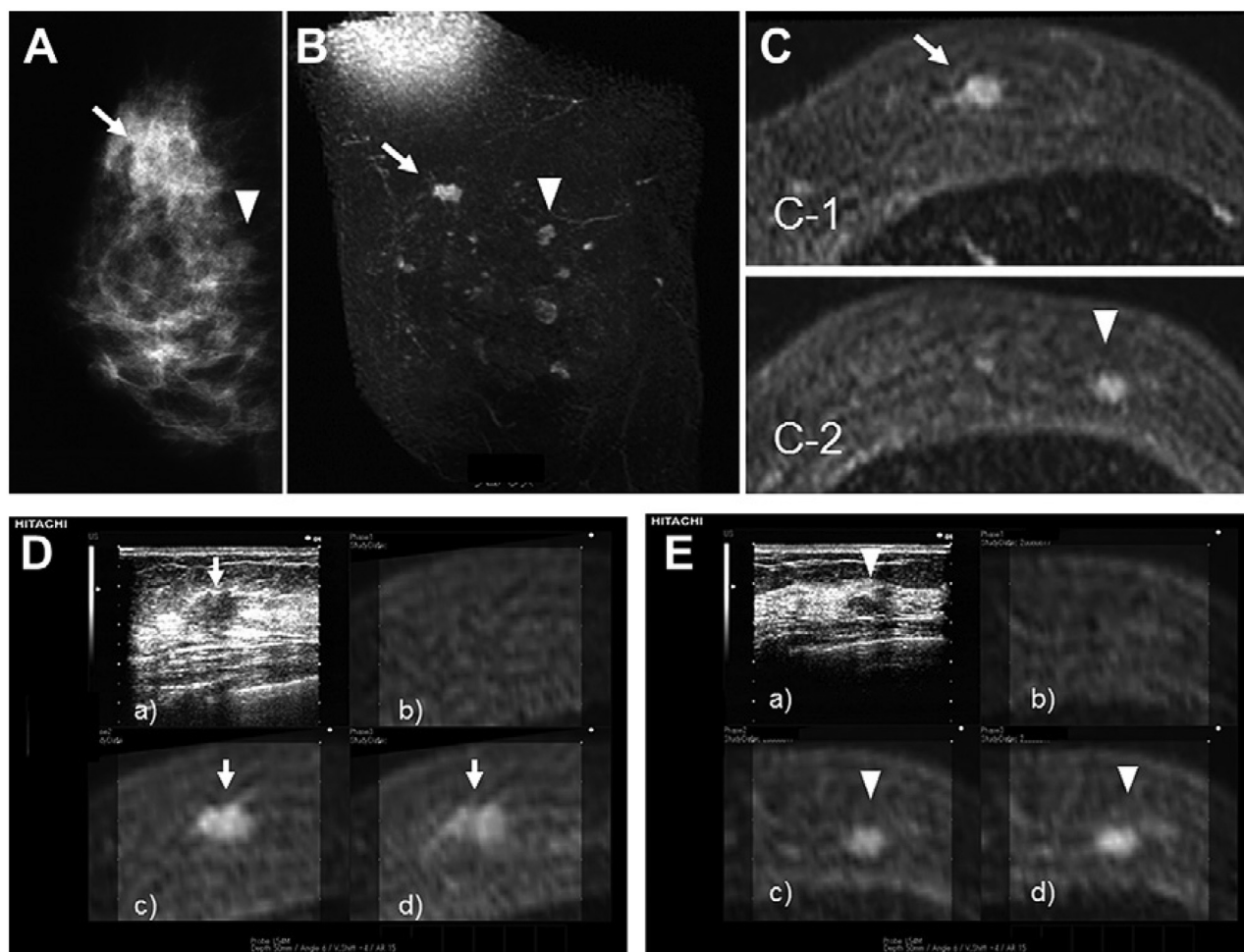


Fig. 15. A 43-year-old patient with architectural distortion and a mass in the right breast. (a) Mammography reveals architectural distortion (*arrow*) and a well-circumscribed mass (*arrowhead*) on the mediolateral oblique films. (b) Coronal T1-weighted, contrast-enhanced magnetic resonance (MR) image. (c) Transverse images reveal an irregularly shaped, margined, 12-mm mass diagnosed as invasive ductal carcinoma (*arrow* in C-1), as well as an oval-shaped, smooth-margined, 8-mm mass that had not been identified on conventional B-mode (*arrowhead* in c-2). (D) Real-time virtual sonography (RVS) reveals a 12-mm, irregularly shaped mass that is taller than it is wide (a), corresponding to the MR lesion (b–d) (*arrow*). The pre-contrast MR image (b) used to identify lesions in the absence of T1-weighted signals before enhancement is necessarily in the image plane displayed by the RVS system. Histopathological analysis of the sonographically guided, core biopsy samples was consistent with invasive ductal carcinoma. (e) RVS reveals an 8-mm oval mass that is wider than it is tall (a), corresponding to the MR lesion (b–d) (*arrowhead*). A histopathological analysis of sonographically guided core biopsy samples indicated that this tumor was a fibroadenoma. Reprinted from Nakano et al. (2012b).

and the sonographic size of the lesions detected by RVS alone was significantly smaller than that of lesions detected by conventional B-mode. Figure 15 illustrates detection of MRI-enhancing lesions with RVS. The overall mean positioning errors from the actual sonographic position to the expected MRI position in the three planes were 7.7, 6.9 and 2.8 mm for the x-, y- and z-planes, respectively. Nakano et al. (2014) reported that coordination by RVS of the present US image with the past US image is a reproducible, operator-independent technique for comparison of US images of BI-RADS category 3 mass lesions obtained at different time points.

Hybrid ultrasound/MRI fusion system. In addition to the navigation systems, there are a few studies that have explored other methods for the co-registration of breast MRI and US. Piron et al. (2003) developed a hybrid biopsy system combining ultrasound and MRI. In this system, the breast was immobilized between lateral and medial compression plates, each supporting a breast MR coil. After pre-biopsy MRI, the MR coils were removed. The lateral fenestrated compression plate is for the biopsy plug, which guides the needle at a defined position and angle. The medial compression plate has acoustical membrane for the US probe. The parameters for the appropriate transducer

position and biopsy-needle trajectory were calculated based on the result of MRI to select the proper needle approach to the lesion. The lesion detected by MRI is identical to the US image. Piron *et al.* (2003) performed an experiment with a breast tissue-mimicking phantom in which the average accuracy scores for MRI/US guidance and MRI guidance alone were 9.6 and 7.4, the average needle correction measured for all MRI/US guidance trials was calculated to be 3.7 mm, and then the hybrid system was completely extended to clinic for two patients in the prone position. The limit is for the tissue near the chest wall. In 2008, their team (Causer *et al.* 2008) subsequently presented the accuracy of the same MRI–sonography co-registration system *in vivo*: the mean lesion size correlated well on MRI (11.4 mm, range: 6–28 mm) compared with that of sonography (10.3 mm, range: 6–28 mm). All three masses were determined to be invasive ductal carcinoma on histopathology. The mean error measurements in the three planes were as follows: 2.5 mm for the x-plane, 1.1 mm for the y-plane and 2.6 mm for the z-plane. This system is currently being developed and is not yet commercially available. Other novel phantoms of the hybrid breast biopsy system combining both modalities with negligible broadband noise and minimal periodic RF noise have been studied (Tang *et al.* 2008).

PET, PET-CT, PEM and CT for breast cancer biopsy and navigating ultrasound-guided biopsy

Positron emission mammography has a high PPV of 0.88 and reveals some breast malignancies not seen on mammograms and/or US images (Berg *et al.* 2006). High-resolution, PEM-guided biopsy has been performed for the sampling of PET-depicted breast lesions in several, published studies (Argus and Mahoney 2014; Kalinyak *et al.* 2011). Recent studies attempted to develop methods with low levels of [^{18}F]fluorodeoxyglucose (FDG) activity, and nearly real-time visualization indicated that PEM could detect a low level of activity of [^{18}F]FDG to decrease the radiation dose (Argus and Mahoney 2014; Choudhery and Seiler 2015). A system of nearly real-time visualization of lesion displacement simulation during the procedure of PEM-guided, breast biopsy has been developed.

Combining FDG PET/CT with US or MRI could improve diagnostic performance for the detection of axillary node metastases compared with that of FDG PET/CT alone (An *et al.* 2014). One study reported the fusion of US-guided navigation with PET/CT to facilitate identification and excision of suspicious axillary lymph node (Futamura *et al.* 2013).

In addition, a pilot study (Kousaka *et al.* 2016) that detected breast lesions with CT-coordinated real-time sonography images suggested that targeted sonography using real-time virtual sonography is a useful technique for identifying incidentally detected breast lesions on chest

CT. Yamamoto *et al.* (2010) reported that US guided by RVS was able to detect all of the same sentinel lymph nodes visualized by CT in 7 of the 60 patients.

Combined ultrasound/mammography-guided biopsy

Surry *et al.* (2007) proposed an alternative dual-modality system that combines stereotactic mammography (SM) imaging for position information with real-time 3-D US imaging for guidance information. The breast probe of the 3-D US-guided biopsy system is mounted on an upright stereotactic mammography unit and with stereotactic mammography for pre-procedural imaging, real-time 2-D and near real-time 3-D US imaging for intra-procedural targeting and guidance and 3-D US imaging for verification of the needle penetrating the target immediately post-biopsy.

Summary

Integrated imaging modalities can potentially compensate the weaknesses of each other. First, ultrasound can reduce the interference of gas, calcification and a variety of artifacts, together with the strength of flexible and real-time ultrasound imaging. Real-time image fusion with ultrasound can be accurately carried out to assess target lesions previously identified by another imaging modality, which may lead to many clinical applications. Second, ultrasound fusion imaging can guide biopsies to the lesions only visible by other modalities and can also avoid the disadvantage of other modalities that the needle and the lesion relationship cannot be tracked in real time. Third, an ultrasound fusion volume navigation technique can be used to scan the breast nodules requiring follow-up. A limitation of real-time image fusion of ultrasound with other modalities may be registration accuracy. This error could be due to the dislocation or deformation of breast tissue and the registration algorithm. New algorithms have been developed for assessing organ motion induced by breathing and movement. More landmarks or a precise electromagnetic tracking system might improve the accuracy. In the next section, we compare the accuracy of ultrasound with that of other imaging modalities for breast cancer diagnosis.

ACCURACY OF OTHER MODALITIES FOR BREAST CANCER DIAGNOSIS

Mammography and ultrasound for breast screening

Digital mammography is an effective universal technique used to decrease breast cancer mortality. Mammographic screening results in a highly significant decrease in breast cancer-specific mortality (Hofvind *et al.* 2013). Long-term outcomes in 2,305,427, screened asymptomatic women (Cutler *et al.* 2015) revealed that the average cumulative incidence rate of the first case of

Table 2. Relative risk of breast cancer mortality with mammography screening

Author(s) and year	Accrual period	Study recruitment	RR of breast cancer mortality ≥ 50 y	RR of breast cancer mortality < 50 y
Nystrom et al. 2002	≤ 1996	247,010 women Invited group 129,750 Control group 117,260	50–54 y: RR = 0.95 55–59 y: RR = 0.76 60–64 y: RR = 0.68 65–69 y: RR = 0.69	—
Bastardis-Zakas et al. 2010	1988–2006	Meta-analyses of 8 randomized control trials	—	40–49 y: RR = 0.81
Moss et al. 2006	1963–1990	160,921 women	—	40–49 y: RR = 0.83 95% CI: 0.66–1.04 $p = 0.11$
Humphrey et al. 2002	1963–1982	Reviewed 154 publications from 10 trials	≥ 50 y: RR = 0.78 95% CI: 0.70–0.87	< 50 y: RR = 0.85 95% CI: 0.73–0.99
Nelson et al. 2009	1986–2006	Meta-analysis of 7 mammography screening trials	50–59 y: RR = 0.86 95% CI: 0.75–0.99 60–69 y: RR = 0.68 95% CI: 0.54–0.87	39–49 y: RR = 0.85 95% CI: 0.75–0.96
Fitzpatrick-Lewis et al. 2011	2008–2010	Systematic review randomized controlled trials	50–69 y: 7 studies RR = 0.79 95% CI: 0.68–0.90 ≥ 70 y: 2 trials RR = 0.68 95% CI: 0.45–1.01	39–49 y: 8 trials RR = 0.85 95% CI: 0.75–0.96 39–49 y: 2 trials RR = 0.97 95% CI: 0.91–1.04
Miller et al. 2014	1980–1985 25-y follow-up	89,835 women, randomized controlled trials	40–59 y: HR = 1.05 95% CI: 0.85–1.30	Findings for women aged 40–49 and 50–59 were almost identical
Hamashima et al. 2015	1985–2014	Randomized controlled trials on PubMed and other databases	40–74 y without clinical breast examination: RR = 0.75 40–64 y with clinical breast examination: RR = 0.87	

CI = confidence interval; HR = Hazard ratio; RR = relative risk.

invasive breast cancer increased by 0.20% each year. With 25 y of follow-up, 94.55% of the patients remained disease free, and an average of 0.23% of the post-menopausal women were diagnosed with a first case of invasive breast cancer each year. The specificity of a single mammographic examination was 94% to 97% (Humphrey et al. 2002).

It is accepted that the relative risk (RR) for women older than 50 screened by mammography has dropped, although the sensitivity of mammography is substantially lower for women in their forties than for older women. The greatest reduction of breast cancer deaths occurred in the age group 60–69 y (33%); statistically significant effects were noted in the age groups 55–59, 60–64 and 65–69 y; and a small effect occurred in women 50–54 y (Nystrom et al. 2002). Mammography has some problems: over 10 y of biennial screening among 40-y-old women invited to be screened, approximately 400 women have false-positive results on mammography and 100 women undergo biopsy or fine-needle aspiration for each death from breast cancer prevented (Humphrey et al. 2002). For a 40- or 50-y-old woman undergoing 10 y of annual mammograms, the cumulative risk of a false-positive result is about 61% (Pace and Keating 2014). We summarize the relative risk of breast cancer mortality with mammography

screening in Table 2. There is some controversy over the age at which screening should start. In November 2009, the U.S. Preventive Services Task Force (USPSTF) recommended biennial screening mammography for women aged 50–74 y. For women before the age of 50, USPSTF recommended that the decision to start regular, biennial screening mammography should be an individual one and the patient's context should be taken into account, including her values regarding specific benefits and harms. But both the American Cancer Society (Saslow et al. 2007) and the American College of Obstetricians and Gynecologists (Corbelli et al. 2014) recommend that mammography be initiated at age 40 and continued annually (Corbelli et al. 2014).

Mammographic sensitivity for breast cancer declines significantly with increasing breast density (Kerlikowske et al. 1996; Kolb et al. 2002; Saarenmaa et al. 2001). More than 40% of women between 25 and 55 y have $> 50\%$ parenchymal density (Stomper et al. 1996), which partly explains why the sensitivity of mammograms is lower for women in their forties than for older women. In 577 new breast cancer patients, breast parenchyma in total breast was dense in 52% of women aged 26–49, in 28% of women aged 50–59 and in 9% of women aged 60–92 (Saarenmaa et al. 2001). The sensitivity of

mammography is just 30% in women with extremely dense breasts (Mandelson et al. 2000). The sensitivity and specificity of screening mammography examinations increase with age, based on Breast Cancer Surveillance Consortium (BCSC) data through 2009 (BCSC 2014b). Moreover, increased mammographic breast density is a moderately independent risk factor for breast cancer in older women. The odds ratio for developing breast cancer for the most dense compared with the least dense breast tissue categories ranges from 1.8 to 6.0 (Harvey and Bovbjerg 2004).

Ultrasound is an extensively used breast imaging modality in the clinical setting; it is relatively inexpensive and has a high degree of patient acceptability. Although in women older than 50, mammography is more sensitive for detecting breast cancer than US (sensitivity of mammography = 0.95, sensitivity of US = 0.85) (Saarenmaa et al. 2001), in women ≤ 45 y the sensitivity of sonography is 13.2% greater than that of mammography (Houssami et al. 2003). US has been reported to have great value as a complementary examination to mammography, especially in younger patients and in patients with mammography-negative and dense breast parenchyma (Corsetti et al. 2008; Crystal et al. 2003; Saarenmaa et al. 2001) and with tumors > 2 cm (Skaane et al. 1999). The combined use of mammography and US has been reported to be an effective tool in the detection of breast cancer. For example, the combination resulted in a sensitivity and specificity of 92.0% and 97.7%, respectively, in an observational follow-up study (Duijm et al. 1997). The diagnostic accuracy of mammography was reported to increase from 0.78 to 0.91 for mammography plus US (Berg et al. 2008). The addition of US for screening significantly increased the detection of small tumors and improved breast cancer detection at a lower stage (Kolb et al. 2002).

MRI for breast cancer diagnosis

Magnetic resonance imaging has a number of morphologic sequences to evaluate breast tissue density and morphologic changes and to assess the condition of the skin, armpits and edge of the pectoral muscle. Breast MRI has the ability to detect malignancy that is clinically and mammographically occult and to provide a NPV that may help to safely exclude a diagnosis of malignancy (Moy et al. 2009). Table 3 compares the diagnostic performance of multimodalities for breast cancer diagnosis. MRI might find a new lesion in breast cancer patients who have been diagnosed. It was reported that MRI made 69 additional findings in 99 patients with breast cancer; of these, 51 findings were true positives, including 16 larger single lesions, 18 cases of multifocality, 7 cases of multicentricity, 3 cases of contralateral lesions and 5 cases of lymph node involvement (Mameri et al. 2008). The additional proportion

of cases detected by MRI was estimated at 16% in meta-analysis (Houssami and Hayes 2009).

Many studies have reported that breast MRI is a promising method for screening young women at high risk for breast cancer (Kriege et al. 2004; Kuhl et al. 2000, 2005; Sardanelli et al. 2007; Tilanus-Linthorst et al. 2000; Warner et al. 2001, 2004). Kuhl et al. (2005) reported that the SE of MRI (90.7%) is significantly higher than that of mammography (39.5%) and ultrasound (36.2%) in carriers of a breast cancer susceptibility gene, whereas the SPs are equivalent. Diagnosis of intra-ductal and invasive breast cancer in familial or hereditary cancer is achieved with a significantly higher SE and at a more favorable stage using MRI surveillance than another modality (Kuhl et al. 2005). In 2007, MRI was recommended by the American Cancer Society Guidelines for breast screening in patients with an approximately 20%–25% or greater lifetime risk of breast cancer, including women with a strong family history of breast or ovarian cancer and women who were treated for Hodgkin's disease (Saslow et al. 2007). However, the SP of MRI is not stable, as 0.37–0.92 (Harms et al. 1993; Leach et al. 2005; Moy et al. 2009) results in the need for further follow-up MRI and biopsy and as overall screening increased the costs, MRI is not the best choice as a breast cancer screening method. Annual screening with MRI and mammography improves metastasis-free survival in women with BRCA1 mutation or a familial predisposition (Saadatmand et al. 2015). Contrast-enhanced MRI might be more a cost-effective screening modality than mammography as well as both strategies combined for women at high risk, particularly for the BRCA1 and BRCA2 subgroups (Griebsch et al. 2006). MRI could help to improve the ability to diagnose DCIS (Morris et al. 2003). MR had a higher SE than mammography for all tumor types and a higher SE than US for DCIS (Berg et al. 2004), especially DCIS of high nuclear grade (Kuhl et al. 2007). Therefore, the indications for MRI are diagnosis of tumor recurrence, screening of high-risk patients, detection of primary tumors in patients with nodal metastases of unknown character, evaluation of the response in patients treated with chemotherapy and analysis of breast implants to rule out rupture (Tejerina Bernal et al. 2012).

Magnetic resonance imaging does not currently seem to be effective in ruling out the need for biopsy in the assessment of sonographic BI-RADS 4 lesions (Sarica and Uluc 2014). When only ultrasonographic BI-RADS 4 lesions are considered, the SP of MRI is 56.7% (Sarica and Uluc 2014). In meta-analysis, the SP of contrast-enhanced MRI in patients with breast lesions is 0.72 (Peters et al. 2008), and the pooled weighted SP of quantitative, diffusion-weighted (DW) MR imaging in patients with breast lesions was 0.84 (Chen et al. 2010). Biopsy is still required to identify true-positive lesions according to the results of breast MRI.

Table 3. Diagnostic performance of multimodality imaging in breast cancer (sensitivity and specificity)

Author and year	Accrual period	No. of subjects	Mammography	Ultrasound	MRI	PET
BCSC data through 2009 (BCSC 2014a)	2004–2008	363,048 diagnostic mammography examinations	SE = 84.4% SP = 91.3%	—	—	—
Kolb et al. 2002	1995–2000	11,130 asymptomatic Mean age: 63.7 y	Total SE = 77.6% ≤49 y: SE = 58% ≥50 y: SE = 82.7% Total SP = 98.8%	Total SE = 75.3% ≤49 y SE = 78.6% ≥50 y SE = 74% Total SP = 96.8%	—	—
Saarenmaa et al. 2001	1996–1997	572 breast cancer cases age groups 26–49, 50–59 and 60–92	SE = 0.93% Increased by age, fattiness of breast OR = 0.2–0.4	SE = 0.86% Decreased by age OR = 2.3 Increased by fattiness of breast OR = 0.5	—	—
Houssami et al. 2003	1994–1996	480 25–55 y 240 with breast cancer 240 age-matched without cancer	Total SE = 75.8% ≤45 y: SE = 71.7% 46–55 y: SE = 79.1% Total SP = 87.6%	Total SE = 81.7% ≤45 y: SE = 84.9% 46–55 y: SE = 79.1% total SP = 88.0%	—	—
Shen et al. 2015	2008–2010	13,339 high-risk women 30–65 y	SE = 57.1% SP = 100% Diagnostic accuracy = 76.6% PPV = 72.7%	SE = 100% SP = 99.9% Diagnostic accuracy = 99.9% PPV = 70.0%	—	—
Berg et al. 2004	1999–2002	177 malignant foci in 121 cancerous breasts	SE = 67.8% SP = 75%	SE = 83.0% SP = 34%	SE = 94.4% SP = 26%	—
Kuhl et al. 2005	1996–2002 mean follow-up of 5.3	529 asymptomatic women who were suspected or proven to have a BRCA	SE = 32.6% SP = 96.8%	SE = 39.5% SP = 90.5%	SE = 90.7% SP = 97.2%	—
Kuhl et al. 2000	1996–1998	192 asymptomatic women proven or suspected to be carriers of a breast cancer susceptibility gene	SE = 33% PPV = 30%	SE = 33% PPV = 12%	SE = 100% PPV = 64%	—
Leach et al. 2005	1997–2004	649 patients with strong family history of breast cancer or high probability of BRCA1, BRCA2 or TP53 mutation	SE = 40% SP = 93%	—	SE = 77% SP = 81%	—
Sardanelli et al. 2011	2000–2007	501 women with high genetic risk	SE = 50% SP = 99%	SE = 52% SP = 98.4%	SE = 91% SP = 96.7%	—
Warner et al. 2008	Databases 1995–2007	Summarized 11 studies that screened women at very high risk for breast cancer	SE = 32% SP = 94.7%	—	SE = 75% SP = 96.1%	—
Zhang et al. 2014	2006–2012	164 patients with invasive breast cancer	—	—	—	SE = 86%
Song et al. 2015	2008–2012	86 patients with invasive breast cancer Detecting multifocality in breast cancer patients	SE = 66.7% SP = 89.5%	SE = 83.3% SP = 71.1%	SE = 100% SP = 61.8%	SE = 33.3 % SP = 93.4 %
Berg et al. 2011	2006–2008	388 women with invasive and/or intra-ductal breast cancer	—	—	SE = 80.7% SP = 86.3% PPV = 53%	For PEM SE = 80.5% SP = 91.2% PPV = 66%
Berg et al. 2006	—	94 consecutive women with known breast cancer	—	—	—	For PEM SE = 90 SP = 86 PPV = 88 NPV = 88 Accuracy = 88

BRCA = breast cancer susceptibility gene; MRI = magnetic resonance imaging; NPV = negative predictive value; OR = odds ratio; PEM = positron emission mammography; PET = positron emission tomography; PPV = positive predictive value; SE = sensitivity; SP = specificity.

CT for breast cancer diagnosis

The value of CT for breast diseases has not yet been fully evaluated. In fact, during routine chest CT examinations, the prevalence of breast cancers among incidental lesions detected varied from 24% to even 70%; therefore, radiologists should pay attention to the breast (Son *et al.* 2016). Furthermore, many scholars have been devoted to the study for dedicated breast CT (DBCT). In 2002, feasibility of cone-beam volume CT breast imaging technique was analyzed based on cone-beam X-ray projection volume imaging (Chen and Ning 2002). Since 2004, researchers have started to develop DBCT systems capable of cone-beam CT and have conducted clinical studies, contrast-enhanced breast CT (CEBCT) and DBCT comfort questionnaire (Lindfors *et al.* 2008).

Prototype breast CT systems make use of flat panel detectors, which give rise to the half-cone beam geometry (Lindfors *et al.* 2010). The average glandular dose (AGD) from breast CT varied from 5 to 15 mGy (O'Connell *et al.* 2014). The mean glandular dose from breast CT corresponds to the mean glandular dose from four or five mammography views, and the mean number of views per breast during diagnostic mammography was 4.53 (Vedantham *et al.* 2013a, 2013b). There were no statistically significant differences between the glandular dose from cone-beam CT and that from mammography (O'Connell *et al.* 2010). Breast tissue coverage of CBCT was better in the lateral, medial and posterior, but inferior in the axilla and axillary tail compared with mammography (O'Connell *et al.* 2010). Vedantham *et al.* (2013a, 2013b) has investigated the system geometry with prone and upright breast CT positioning and achieved posterior breast coverage equivalent to that provided by mammograms. Comparisons between DBCT and other breast modalities are reported in a review paper (O'Connell *et al.* 2014). In digital breast tomosynthesis, the ability of separating the slices varies depending on object diameter and the arc span, whereas in DBCT it is stable. The scan time of DBCT is 10 s and a bilateral CEBCT can be done within a few min. Single injection of contrast media can complete bilateral CEBCT (O'Connell *et al.* 2014). DBCT usually scans one breast at a time and requires patient repositioning for a bilateral examination. DBCT can detect all masses detected by mammography (O'Connell *et al.* 2010) and significantly improves visualization in shape and margin of suspicious masses (Kuzmiak *et al.* 2016), especially in patients with dense breast tissue (Wienbeck *et al.* 2017a), but detection of calcifications is controversial. Kuzmiak *et al.* (2016) has shown the reader confidence that calcification with CBCT was reduced. In another study, cone-beam breast computed tomography (CBBCT) accurately distinguished DCIS from benign causes of microcalcifications compared with mammography. (Wienbeck *et al.* 2017b)

A prospective study of 110 pathologically confirmed lesions revealed that DBCT provided high-quality images of the breast and could help radiologists to diagnose malignant breast lesions, compared with ultrasound and digital mammography (He *et al.* 2016). In a recent study, DBCT was used to identify breast lesions and was compared with BI-RADS Mammography Atlas; the estimated overall sensitivity of the readers was 0.969, and the specificity was 0.529 (Jung *et al.* 2017a, 2017b).

Contrast-enhanced breast CT could increase the conspicuity of benign and malignant masses and has potential in evaluating the extent of disease and monitoring chemotherapy (O'Connell *et al.* 2014). As for molecular and pathologic type, Ki-67, ER, PR and HER2 did not correlate with CT density of breast cancer. Tubular carcinoma tended to have a higher CT density in comparison to other subtypes of breast carcinoma (Wienbeck *et al.* 2017b).

PET, PET-CT and PEM for breast cancer diagnosis

Positron emission tomography, one of the most frequently used tumor imaging modalities, quantitatively presents metabolic activity to reflect lesion characterization and to contribute to treatment planning. FDG PET imaging screens the entire patient for local recurrences, lymph node metastases and distant metastases and, at a relatively low detection rate, bone metastases (Lind *et al.* 2004). PET scans have a high positive predictive value (96.6%) for patients suspected of having primary breast cancer (Avril *et al.* 2000). Partial volume effects and varying metabolic activity, depending on the tumor type, seem to represent the most significant limitations to the routine diagnostic application of PET (Avril *et al.* 2000). Breast cancers with higher SUV can be overestimated because of the overflow effect, whereas small cancers with lower SUV can be underestimated because of the partial volume effect. With respect to breast tumor size, the accuracy of FDG PET (43.5%) is significantly lower than that of MRI (91%) (Uematsu *et al.* 2009). Tumor histology may influence the usefulness of FDG PET/CT for systemic staging of patients with breast cancer. For instance, invasive lobular carcinoma would have a greater possibility of non-FDG-avid sclerotic osseous metastases than invasive ductal carcinoma (Dashevsky *et al.* 2015). FDG-PET has a very low SE (33.33%) for invasive breast cancers even though it has a high SP (93.42%).

Positron emission tomography-computed tomography (PET-CT) allows the merging of morphologic and functional images. The rather low SP of FDG PET for breast cancer can be improved by utilizing combined anatomic-molecular imaging techniques, such as PET/CT tomography (Lind *et al.* 2004). Whole-body PET-CT is extremely useful in tumor staging at a distance; especially in advanced stage breast cancer cases and also has a role in locoregional lymph-node staging. Distant

metastases were detected with FDG PET/CT in 100% (Heusner et al. 2008). Riedl et al. (2014) suggested that PET/CT might be valuable in younger patients with stage IIB and III disease. The patient-based SE and SP of FDG PET/CT were 96% and 89%, respectively (Lind et al. 2004). Although the SE was similar to that in their previous study using FDG PET alone, the SP was significantly higher for PET/CT (Lind et al. 2004). The other research studies reported that the SE of PET/CT and US for the diagnosis of breast cancer were 86% and 91%, respectively (He et al. 2015). As PET/CT is very expensive and not superior to US for detecting primary breast cancer, it cannot be recommended as the primary diagnostic procedure for early breast cancer (He et al. 2015).

Positron emission mammography is a high spatial resolution tomographic method for molecular imaging of positron-emitting isotopes. PEM was approved by the U.S. FDA and has been introduced into clinical use as a diagnostic adjunct to mammography and breast ultrasonography. PEM detected more newly diagnosed breast tumors (92%) than whole-body PET (56 %) or PET/CT (87%) (Kalinyak et al. 2014). PEM and MR imaging had comparable breast-level SEs (Kalles et al. 2013), that is, 80.5% and 80.7% for all breast malignancies and 51% and 60% for additional foci of tumor, respectively (Berg et al. 2011); in addition, the SP of PEM (91.2%) is higher than that for MR imaging (86.3%) (Berg et al. 2011).

Summary

Imaging modalities for detection of breast cancers have been continuously improved and upgraded with new techniques, leading to improved diagnostic performance and reduced false-negative rates. In the era of personalized medicine, doctors' knowledge regarding various imaging technologies will help in selection of the most accurate diagnostic method suitable for breast cancer diagnosis. In addition to breast cancer biopsy and diagnosis, ultrasound has also been used for detecting lymph node metastasis as discussed next.

ULTRASOUND AND OTHER MODALITIES FOR LYMPH NODE DIAGNOSIS

Axillary lymph node metastasis is closely related to the prognosis of breast cancer. However, determination of the status of lymph nodes cannot rely on clinical examination as many lymph node metastases are not palpable. Ultrasonography is used to assess axillary lymph nodes with respect to their size, shape, cortical thickness and echo, to determine their status (American College of Radiology (ACR) 2015; Lee et al. 2008; Skaane and Skjorten 1999). A node is confirmed to be abnormal based on the following ultrasound features: oval to rounded shape; hypoechoic appearance with the absence of fatty hilum; eccentric

cortical hypertrophy; lobulation; and a diameter larger than 4–5 mm. Pre-operative, axillary ultrasound is crucial for the staging and management of breast cancer in many clinical institutions (Gentilini and Veronesi 2012), and it can detect some metastases and reduce the number of false-negative biopsies. In addition, MRI and FDG PET/CT can act as selected candidates for predicting sentinel lymph node biopsy. We present the major published results regarding the diagnostic performance of difference imaging modalities for detecting breast lymph nodes (Table 4). FDG PET imaging screens patients with breast cancer for lymph node metastases with a reported average SE of 47.7%–92.2% and SP of 81.6%–92%. The diagnostic accuracy of PET/CT is correlated with axillary lymph node size (Zhang et al. 2014). Some studies have found that the presence of internal mammary (IM) lymph node metastasis is a useful prognostic indicator and that IM metastasis has been associated with higher rates of distant disease and lower overall patient survival rates (Cody and Urban 1995; Sugg et al. 2000). PET has excellent performance in evaluating internal mammary lymph node metastasis (SE = 0.85, SP = 0.90, accuracy = 0.88) (Eubank et al. 2001).

Sentinel lymph nodes (SLNs) can be an accurate predictor of the status of the axillary nodes. Currently, sentinel lymph node biopsy (SLNB) has become the standard alternative for axillary lymph node dissection (ALND) for assessing axillary lymph node stages and reducing post-operative complications in breast cancer patients (Mansel et al. 2006; Naik et al. 2004). The National Surgical Adjuvant Breast and Bowel Project (NSABP) Trial B-32 found that overall patient survival, disease-free survival and regional control were statistically equivalent between the SLN resection plus ALND group and the SLN resection-alone group, which explained that when the SLN is negative, SLN surgery alone with no further ALND is an appropriate, tolerable and effective therapy for breast cancer patients with clinically negative lymph nodes (Krag et al. 2010), even in small breast cancers ≤ 2 cm in diameter (Veronesi et al. 2003). For comparison of the axillary lymph node extent between patients with positive nodes determined using ultrasound-guided needle biopsy (USNB) and positive nodes on SLNB, Boone et al. (2015) reported that breast cancer patients with a positive node detected on ultrasound-guided biopsy have a significantly greater possibility of axillary disease than patients with a positive sentinel lymph node. In any case, ultrasound-detected abnormal lymph nodes can be histologically confirmed by ultrasound-guided biopsy to reduce unnecessary SLNB or even ALND and maximally invasive radical resection (Moorman et al. 2014).

As reported in the literature, 3-D multidetector-row CT lymphography using iopamidol is a reliable method for the pre-operative detection of SLNs and the prediction of SLN metastasis in breast cancer patients (Suga et al. 2005).

Table 4. Diagnostic performance of multiple imaging modalities in breast lymph nodes

Author and year	Accrual period	No. of subjects	Mammography		Ultrasound		MRI	PET
Zhang <i>et al.</i> 2015	2010–2011	1049 breast cancers	—		SE = 69.4 SP = 81.8 Accuracy = 77		—	—
Xin <i>et al.</i> 2014	2012–2013	323 females with primary breast cancer	—		SE = 35.6 SP = 98.9 PPV = 35.6 NPV = 68.3		—	—
Alvarez <i>et al.</i> 2006	1980–2004	Meta-analysis with 16 articles	—	Criterion Size: > 5 mm	Non-palpable SE = 48.8–87.7 SP = 55.6–97.3	Palpable + non-palpable SE = 66.1–72.7 SP = 44.1–97.9	—	—
				Morphology	SE = 26.4–75.9 SP = 88.4–98.1	SE = 54.7–92.3 SP = 80.4–87.1		
Valente <i>et al.</i> 2012	2008–2010	244 invasive breast carcinomas	SE = 21 SP = 99.5	SE = 43.5 SP = 96.2			SE = 37.1 SP = 96.7	—
Heusner <i>et al.</i> 2009	2007–2008	61 patients with breast cancer	—		—		—	FDG PET/CT SE = 58 SP = 92 PPV = 82 NPV = 77 Accuracy = 79
Kvistad <i>et al.</i> 2000	1998	65 patients with invasive breast cancer	—		—		SE = 83 SP = 90 Accuracy = 88	—
Lind <i>et al.</i> 2004	Review of 1989–2004	201	—		—		—	For local recurrence, lymph node metastases and distant metastases SE = 96% SP = 77% FDG-PET SE = 47.7 SP = 81.6 FDG PET/CT SE = 0.80 SE = 92.9
Song <i>et al.</i> 2015	2008–2012	86 invasive breast cancers	SE = 36.4 SP = 86.8		SE = 61.4 SP = 92.1		SE = 61.4 SP = 73.7	
Heusner <i>et al.</i> 2008	—	40 women with suspected breast cancer	—		—		—	
An <i>et al.</i> 2015	2008–2012	37 patients with breast cancer For internal mammary LN metastasis	—		Initial US SE = 76.6 Initial US combined with second-look ultrasound: SE = 96.7		—	

FDG = [¹⁸F]]fluorodeoxyglucose; LN = lymph node; MRI = magnetic resonance imaging; NPV = negative predictive value; OR = odds ratio; PEM = positron emission mammography; PET = positron emission tomography; PPV = positive predictive value; SE = sensitivity; SP = specificity.

Yamamoto et al. (2010) use a 3-D CT lymphography system-guided US to identify SLNs in breast cancer patients. All seven SLNs visualized by 3-D CT lymphography can be detected using the RVS system and 4 of 7 were confirmed as metastases. The virtual multiplanar reconstruction image of the SLN was displayed in synchronization with the US image. SLN metastases were assessed by the shape and visibility of the hilum. Yamamoto et al. (2012) also reported that if the cortical thickness of the SLN is >2.5 mm, the detection accuracy of the real-time, virtual sonography systems could increase (Yamamoto et al. 2012).

In several other studies (Mi et al. 2010; Wang et al. 2009; Zhong et al. 2007), ultrasound contrast agents were injected subcutaneously surrounding breast lesion, and then the degree and pattern of SLN enhancement were observed before methylene blue staining and resection. Because of hypoperfusion of pathologic identified metastases, SLNs have appeared asymmetrically enhanced and a few have been enhanced to a low degree. A validation and quantitative method needs to be developed to differentiate metastatic SLNs confidently.

CONCLUSIONS AND FUTURE DIRECTIONS

In this review, we provide a broad overview of ultrasound imaging techniques for breast cancer detection and ultrasound-guided biopsy and fusion with other modalities. These techniques are of great importance in diagnosing breast lesions as benign or malignant and can further improve early breast cancer detection. This review could serve as a tutorial for medical residents, junior radiologists and researchers who are interested in breast cancer imaging and detection. The limitation of this review is that we have not addressed every aspect of ultrasound imaging for breast cancer in detail.

For breast cancer screening, ultrasound has been applied as an adjunct to mammography. Hand-held ultrasound for the whole breast is time consuming. A large pendulous breast increases the difficulties of ultrasound examinations. Although more breast lesions could be found, most of them are benign (Lashkari et al. 2016), which increases the false-positive rate of breast cancer screening and increases biopsy recommendations in screening (Health Quality Ontario 2016). For breast cancer detection and diagnosis, among many new techniques, breast ultrasound provides quite useful and comprehensive information, including lymph nodes in the axilla, between the pectoral muscles and in the subclavian region, the neck and the medial thoracic chain. The flexibility of ultrasound is superior to that of other modalities, and this advantage is prominent on biopsy, follow-up and fusion with other modalities. Techniques for detecting breast tumor morphology and metabolic activities are constantly improving. Therefore, it is necessary to integrate new technologies for breast

cancer diagnosis and treatment services. CAD makes ultrasonic quantitative analysis possible and provides a reliable and operator-independent technique for breast ultrasound diagnosis. In the future, effective CAD algorithms need to be validated widely in clinical practice. With knowledge of the correlation between the sonographic features and pathologic molecular markers and with the development of targeted contrast agents, breast ultrasound may provide molecular diagnosis in the future.

Acknowledgments—This work was partially supported by National Institutes of Health (NIH) Grants CA156775, CA176684 and CA204254 and a Georgia Research Alliance Distinguished Scientists Award.

REFERENCES

- Alvarez S, Aorbe E, Alcorta P, López F, Alonso I, Corts J. Role of sonography in the diagnosis of axillary lymph node metastases in breast cancer: A systematic review. *AJR Am J Roentgenol* 2006; 186:1342–1348.
- American College of Radiology (ACR). BI-RADS, 5th ed. Reston, VA: Author; 2015. Available at: https://www.acr.org/-/media/ACR/Documents/PDF/QualitySafety/Resources/BIRADS/Posters/BIRADS-Reference-Card_web_F.pdf?la=en. Accessed December 16, 2015.
- An YS, Lee DH, Yoon JK, Lee SJ, Kim TH, Kang DK, Kim KS, Jung YS, Yim H. Diagnostic performance of 18F-FDG PET/CT, ultrasonography and MRI: Detection of axillary lymph node metastasis in breast cancer patients. *Nuklearmedizin* 2014;53:89–94.
- An YY, Kim SH, Kang BJ, Lee AW. Comparisons of positron emission tomography/computed tomography and ultrasound imaging for detection of internal mammary lymph node metastases in patients with breast cancer and pathologic correlation by ultrasound-guided biopsy procedures. *J Ultrasound Med* 2015;34:1385–1394.
- Argus A, Mahoney MC. Positron emission mammography: Diagnostic imaging and biopsy on the same day. *AJR Am J Roentgenol* 2014; 202:216–222.
- Athanasiou A, Tardivon A, Tanter M, Sigal-Zafrani B, Bercoff J, Deffieux T, Gennisson JL, Fink M, Neuenschwander S. Breast lesions: Quantitative elastography with supersonic shear imaging—Preliminary results. *Radiology* 2010;256:297–303.
- Avril N, Rose CA, Schelling M, Dose J, Kuhn W, Bense S, Weber W, Ziegler S, Graeff H, Schwaiger M. Breast imaging with positron emission tomography and fluorine-18 fluorodeoxyglucose: Use and limitations. *J Clin Oncol* 2000;18:3495–3502.
- Bai M, Du L, Gu J, Li F, Jia X. Virtual Touch tissue quantification using acoustic radiation force impulse technology: Initial clinical experience with solid breast masses. *J Ultrasound Med* 2012;31:289–294.
- Balleysguier C, Ayadi S, Van Nguyen K, Vanel D, Dromain C, Sigal R. BI-RADS classification in mammography. *Eur J Radiol* 2007;61: 192–194.
- Balleysguier C, Opolon P, Mathieu MC, Athanasiou A, Garbay JR, Delalogue S, Dromain C. New potential and applications of contrast-enhanced ultrasound of the breast: Own investigations and review of the literature. *Eur J Radiol* 2009;69:14–23.
- Bamber J, Cosgrove D, Dietrich C, Fromageau J, Bojunga J, Calliada F, Cantisani V, Correia J, D'Onofrio M, Drakonaki E. EFSUMB guidelines and recommendations on the clinical use of ultrasound elastography: Part 1. Basic principles and technology. *Ultraschall Med* 2013;34:169–184.
- Barr RG. Sonographic breast elastography: A primer. *J Ultrasound Med* 2012;31:773–783.
- Bastardis-Zakas K, Iatrakis G, Navrozoglou I, Peitsidis P, Salakos N, Malakassis P, Zervoudis S. Maximizing the benefits of screening mammography for women 40–49 years old. *Clin Exp Obstet Gynecol* 2010; 37:278–282.

- Berg WA, Blume JD, Cormack JB, Mendelson EB, Lehrer D, Bohm-Velez M, Pisano ED, Jong RA, Evans WP, Morton MJ, Mahoney MC, Larsen LH, Barr RG, Farria DM, Marques HS, Boparai K. Combined screening with ultrasound and mammography vs mammography alone in women at elevated risk of breast cancer. *JAMA* 2008;299:2151–2163.
- Berg WA, Cosgrove DO, Dore CJ, Schafer FK, Svensson WE, Hooley RJ, Ohlinger R, Mendelson EB, Balu-Maestro C, Locatelli M, Tourasse C, Cavanaugh BC, Juhan V, Stavros AT, Tardivon A, Gay J, Henry JP, Cohen-Bacrie C. Shear-wave elastography improves the specificity of breast US: The BE1 multinational study of 939 masses. *Radiology* 2012;262:435–449.
- Berg WA, Gutierrez L, NessAiver MS, Carter WB, Bhargavan M, Lewis RS, Ioffe OB. Diagnostic accuracy of mammography, clinical examination, US, and MR imaging in preoperative assessment of breast cancer. *Radiology* 2004;233:830–849.
- Berg WA, Madsen KS, Schilling K, Tartar M, Pisano ED, Larsen LH, Narayanan D, Ozonoff A, Miller JP, Kalinyak JE. Breast cancer: Comparative effectiveness of positron emission mammography and MR imaging in presurgical planning for the ipsilateral breast. *Radiology* 2011;258:59–72.
- Berg WA, Mendelson EB, Cosgrove DO, Doré CJ, Gay J, Henry J-P, Cohen-Bacrie C. Quantitative maximum shear-wave stiffness of breast masses as a predictor of histopathologic severity. *AJR Am J Roentgenol* 2015;205:448–455.
- Berg WA, Weinberg IN, Narayanan D, Lobrano ME, Ross E, Amodei L, Tafta L, Adler LP, Uddo J, Stein W. High-resolution fluorodeoxyglucose positron emission tomography with compression (“positron emission mammography”) is highly accurate in depicting primary breast cancer. *Breast J* 2006;12:309–323.
- Bhatti PT, LeCarpentier GL, Roubidoux MA, Fowlkes JB, Helvie MA, Carson PL. Discrimination of sonographically detected breast masses using frequency shift color Doppler imaging in combination with age and gray scale criteria. *J Ultrasound Med* 2001;20:343–350.
- Bluvol N, Kornecki A, Shaikh A, Del Rey Fernandez D, Taves DH, Fenster A. Freehand versus guided breast biopsy: Comparison of accuracy, needle motion, and biopsy time in a tissue model. *AJR Am J Roentgenol* 2009;192:1720–1725.
- Boone BA, Huynh C, Spangler ML, Sumkin J, Johnson R, McGuire KP, Soran A, Ahrendt GM. Axillary lymph node burden in invasive breast cancer: A comparison of the predictive value of ultrasound-guided needle biopsy and sentinel lymph node biopsy. *Clin Breast Cancer* 2015;15:e243–e248.
- Breast Cancer Surveillance Consortium (BCSC). Sensitivity and specificity by indication for examination for 363,048 diagnostic mammography examinations from 2004–2008—Based on BCSC data through 2009. Available at: <http://www.bcs-research.org/statistics/benchmarks/diagnostic/2009/tableSensSpec.html>; 2014a. Accessed December 16, 2015.
- Breast Cancer Surveillance Consortium (BCSC). Performance measures for 1,838,372 screening mammography examinations from 2004 to 2008 by age—Based on BCSC data through 2009. Available at: http://www.bcs-research.org/statistics/performance/screening/2009/perf_age.html; 2014b. Accessed December 16, 2015.
- Burbank F. Stereotactic breast biopsy of atypical ductal hyperplasia and ductal carcinoma in situ lesions: Improved accuracy with directional, vacuum-assisted biopsy. *Radiology* 1997;202:843–847.
- Cai L, Wang X, Wang Y, Guo Y, Yu J, Wang Y. Robust phase-based texture descriptor for classification of breast ultrasound images. *Biomed Eng Online* 2015;14:26.
- Calliada F, Campani R, Bottinelli O, Bozzini A, Sommaruga MG. Ultrasound contrast agents: Basic principles. *Eur J Radiol* 1998;27(suppl 2):S157–S160.
- Candelaria R, Fornage BD. Second-look US examination of MR-detected breast lesions. *J Clin Ultrasound* 2011;39:115–121.
- Caproni N, Marchisio F, Pecchi A, Canossi B, Battista R, D’Alimonte P, Torricelli P. Contrast-enhanced ultrasound in the characterisation of breast masses: Utility of quantitative analysis in comparison with MRI. *Eur Radiol* 2010;20:1384–1395.
- Carlsen JF, Ewertsen C, Lönn L, Nielsen MB. Strain elastography ultrasound: An overview with emphasis on breast cancer diagnosis. *Diagnostics (Basel)* 2013;3:117–125.
- Causar PA, Piron CA, Jong RA, Plewes DB. Preliminary in vivo validation of a dedicated breast MRI and sonographic coregistration imaging system. *AJR Am J Roentgenol* 2008;191:1203–1207.
- Chae EY, Shin HJ, Kim HJ, Yoo H, Baek S, Cha JH, Kim HH. Diagnostic performance of automated breast ultrasound as a replacement for a hand-held second-look ultrasound for breast lesions detected initially on magnetic resonance imaging. *Ultrasound Med Biol* 2013;39:2246–2254.
- Chang RF, Hou YL, Lo CM, Huang CS, Chen JH, Kim WH, Chang JM, Bae MS, Moon WK. Quantitative analysis of breast echotexture patterns in automated breast ultrasound images. *Med Phys* 2015;42:4566.
- Chen B, Ning R. Cone-beam volume CT breast imaging: Feasibility study. *Med Phys* 2002;29:755–770.
- Chen L, Chen Y, Diao XH, Fang L, Pang Y, Cheng AQ, Li WP, Wang Y. Comparative study of automated breast 3-D ultrasound and hand-held B-mode ultrasound for differentiation of benign and malignant breast masses. *Ultrasound Med Biol* 2013;39:1735–1742.
- Chen X, Li WL, Zhang YL, Wu Q, Guo YM, Bai ZL. Meta-analysis of quantitative diffusion-weighted MR imaging in the differential diagnosis of breast lesions. *BMC Cancer* 2010;10:1.
- Cheng H, Shan J, Ju W, Guo Y, Zhang L. Automated breast cancer detection and classification using ultrasound images: A survey. *Pattern Recogn* 2010;43:299–317.
- Choudhery S, Seiler S. Positron emission mammography imaging with low activity fluorodeoxyglucose and novel utilization in core-needle biopsy sampling. *World J Nucl Med* 2015;14:63–65.
- Cody HS, III, Urban JA. Internal mammary node status: A major prognosticator in axillary node-negative breast cancer. *Ann Surg Oncol* 1995;2:32–37.
- Corbelli J, Borrero S, Bonnema R, McNamara M, Kraemer K, Rubio D, Karpov I, McNeil M. Physician adherence to U.S. Preventive Services Task Force mammography guidelines. *Womens Health Issues* 2014;24:e313–e319.
- Corsetti V, Houssami N, Ferrari A, Ghirardi M, Bellarosa S, Angelini O, Bani C, Sardo P, Remida G, Galligioni E, Ciatto S. Breast screening with ultrasound in women with mammography-negative dense breasts: Evidence on incremental cancer detection and false positives, and associated cost. *Eur J Cancer* 2008;44:539–544.
- Crystal P, Strano SD, Shcharynski S, Koretz MJ. Using sonography to screen women with mammographically dense breasts. *AJR Am J Roentgenol* 2003;181:177–182.
- Curiel L, Chopra R, Hynynen K. Progress in multimodality imaging: Truly simultaneous ultrasound and magnetic resonance imaging. *IEEE Trans Med Imaging* 2007;26:1740–1746.
- Cutler W, Burki RE, Kolter JS, Chambliss C, Friedmann E. breast cancer incidence in 2,305,427 screened asymptomatic women: Long-term outcomes during menopause [307]. *Obstet Gynecol* 2015;125:98S.
- del Cura JL, Elizagaray E, Zabala R, Legórburu A, Grande D. The use of unenhanced Doppler sonography in the evaluation of solid breast lesions. *Am J Roentgenol* 2005;184:1788–1794.
- Dahabreh IJ, Wieland LS, Adam GP, Halladay C, Lau J, Trikalinos TA. Core needle and open surgical biopsy for diagnosis of breast lesions: An update to the 2009 report. *Comparative Effectiveness Reviews*, No. 139. Rockville, MD: Agency for Healthcare Research and Quality; 2014.
- Dashevsky BZ, Goldman DA, Parsons M, Gönen M, Corben AD, Jochelson MS, Hudis CA, Morrow M, Ulaner GA. Appearance of untreated bone metastases from breast cancer on FDG PET/CT: Importance of histologic subtype. *Eur J Nucl Med Mol Imaging* 2015;42:1666–1673.
- Delle Chiaie L, Terinde R. Three-dimensional ultrasound-validated large-core needle biopsy: Is it a reliable method for the histological assessment of breast lesions? *Ultrasound Obstet Gynecol* 2004;23:393–397.
- Dennison G, Anand R, Makar SH, Pain JA. A prospective study of the use of fine-needle aspiration cytology and core biopsy in the diagnosis of breast cancer. *Breast J* 2003;9:491–493.

- Destounis S, Arieno A, Somerville PA, Seifert PJ, Murphy P, Morgan R, Skolny M, Hanson S, Young W. Community-based practice experience of unsuspected breast magnetic resonance imaging abnormalities evaluated with second-look sonography. *J Ultrasound Med* 2009;28:1337–1346.
- DeSantis C, Ma J, Bryan L, Jemal A. Breast cancer statistics, 2013. *CA Cancer J Clin* 2014;64:52–62.
- Duijm LE, Guit GL, Zaat JO, Koomen AR, Willebrand D. Sensitivity, specificity and predictive values of breast imaging in the detection of cancer. *Br J Cancer* 1997;76:377–381.
- Duncan W, Kerr GR. The curability of breast cancer. *Br Med J* 1976; 2:781–783.
- Eubank WB, Mankoff DA, Takasugi J, Vesselle H, Eary JF, Shanley TJ, Gralow JR, Charlop A, Ellis GK, Lindsley KL, Austin-Seymour MM, Funkhouser CP, Livingston RB. 18-Fluorodeoxyglucose positron emission tomography to detect mediastinal or internal mammary metastases in breast cancer. *J Clin Oncol* 2001;19:3516–3523.
- Evans A, Whelehan P, Thomson K, McLean D, Brauer K, Purdie C, Baker L, Jordan L, Rauchhaus P, Thompson A. Invasive breast cancer: Relationship between shear-wave elastographic findings and histologic prognostic factors. *Radiology* 2012;263:673–677.
- Evans A, Whelehan P, Thomson K, McLean D, Brauer K, Purdie C, Jordan L, Baker L, Thompson A. Quantitative shear wave ultrasound elastography: Initial experience in solid breast masses. *Breast Cancer Res* 2010;12:R104.
- Ewertsen C, Săftoiu A, Gruionu LG, Karstrup S, Nielsen MB. Real-time image fusion involving diagnostic ultrasound. *Am J Roentgenol* 2013;200:W249–W255.
- Fausto A, Rizzatto G, Preziosa A, Gaburro L, Washburn MJ, Rubello D, Volterrani L. A new method to combine contrast-enhanced magnetic resonance imaging during live ultrasound of the breast using volume navigation technique: A study for evaluating feasibility, accuracy and reproducibility in healthy volunteers. *Eur J Radiol* 2012; 81:e332–e337.
- Fausto A, Rubello D, Carboni A, Mastellari P, Chondrogiannis S, Volterrani L. Clinical value of relative quantification ultrasound elastography in characterizing breast tumors. *Biomed Pharmacother* 2015;75:88–92.
- Feng S, Lotz T, Chase JG, Hann CE. An image based vibration sensor for soft tissue modal analysis in a Digital Image Elasto Tomography (DIET) system. *Conf Proc IEEE Eng Med Biol Soc* 2010;2010: 25–28.
- Fitzpatrick-Lewis D, Hodgson N, Ciliska D, Peirson L, Gauld M, Liu YY. Breast cancer—Systematic review. Breast cancer screening. The Canadian Task Force on Preventive Health Care website. Available at: <http://www.cma.ca/content/183/17/1991.full/>; 2011.
- Forsberg F, Goldberg BB, Merritt CR, Parker L, Maitino AJ, Palazzo JJ, Merton DA, Schultz SM, Needleman L. Diagnosing breast lesions with contrast-enhanced 3-dimensional power Doppler imaging. *J Ultrasound Med* 2004;23:173–182.
- Futamura M, Morimitsu K, Nawa M, Kanematsu M, Gotoh N, Yoshida K. Novel navigation surgery using image fusion of PET/CT and sonography for axillary neoplasm: First experience. *Int J Surg Case Rep* 2013;4:719–722.
- Gentilini O, Veronesi U. Abandoning sentinel lymph node biopsy in early breast cancer? A new trial in progress at the European Institute of Oncology of Milan (SOUND: Sentinel node vs observation after axillary ultrasound). *Breast* 2012;21:678–681.
- Gheonea IA, Stoica Z, Bondari S. Differential diagnosis of breast lesions using ultrasound elastography. *Indian J Radiol Imaging* 2011;21: 301–305.
- Giuseppetti GM, Martegani A, Di Cioccio B, Baldassarre S. Elastasonography in the diagnosis of the nodular breast lesions: Preliminary report. *Radiol Med* 2005;110:69–76.
- Goddi A, Bonardi M, Alessi S. Breast elastography: A literature review. *J Ultrasound* 2012;15:192–198.
- Gokhale S. Ultrasound characterization of breast masses. *Indian J Radiol Imaging* 2009;19:242–247.
- Gomez W, Pereira WC, Infantosi AF. Analysis of co-occurrence texture statistics as a function of gray-level quantization for classifying breast ultrasound. *IEEE Trans Med Imaging* 2012;31:1889–1899.
- Griebisch I, Brown J, Boggis C, Dixon A, Dixon M, Easton D, Eeles R, Evans DG, Gilbert FJ, Hawnaur J, Kessar P, Lakhani SR, Moss SM, Nerurkar A, Padhani AR, Pointon LJ, Potterton J, Thompson D, Turnbull LW, Walker LG, Warren R, Leach MO. Cost-effectiveness of screening with contrast enhanced magnetic resonance imaging vs X-ray mammography of women at a high familial risk of breast cancer. *Br J Cancer* 2006;95:801–810.
- Hamashima C, Ohta K, Kasahara Y, Katayama T, Nakayama T, Honjo S, Ohnuki K. A meta-analysis of mammographic screening with and without clinical breast examination. *Cancer Sci* 2015;106:812–818.
- Harms SE, Flamig DP, Hesley KL, Meiches MD, Jensen RA, Evans WP, Savino DA, Wells RV. MR imaging of the breast with rotating delivery of excitation off resonance: Clinical experience with pathologic correlation. *Radiology* 1993;187:493–501.
- Harvey JA, Bovbjerg VE. Quantitative assessment of mammographic breast density: Relationship with breast cancer risk. *Radiology* 2004; 230:29–41.
- He N, Wu YP, Kong Y, Lv N, Huang ZM, Li S, Wang Y, Geng ZJ, Wu PH, Wei WD. The utility of breast cone-beam computed tomography, ultrasound, and digital mammography for detecting malignant breast tumors: A prospective study with 212 patients. *Eur J Radiol* 2016; 85:392–403.
- He X, Shao M, Huo Y, Sun L, Ma C. A comparative study of ¹⁸F-FDG PET/CT and ultrasonography in the diagnosis of breast cancer and axillary lymph node metastasis. *Q J Nucl Medicine Mol Imaging* 2015; 61:429–437.
- Health Quality Ontario. Ultrasound as an adjunct to mammography for breast cancer screening: A health technology assessment. *Ont Health Technol Assess Ser* 2016;16:1–71.
- Helbich TH, Rudas M, Haitel A, Kohlberger PD, Thurnher M, Gnant M, Wunderbaldinger P, Wolf G, Mostbeck GH. Evaluation of needle size for breast biopsy: Comparison of 14-, 16-, and 18-gauge biopsy needles. *AJR Am J Roentgenol* 1998;171:59–63.
- Heusner TA, Kuemmel S, Hahn S, Koeninger A, Otterbach F, Hamami ME, Kimmig KR, Forsting M, Bockisch A, Antoch G. Diagnostic value of full-dose FDG PET/CT for axillary lymph node staging in breast cancer patients. *Eur J Nucl Med Mol Imaging* 2009;36:1543–1550.
- Heusner TA, Kuemmel S, Umutlu L, Koeninger A, Freudenberg LS, Hauth EA, Kimmig KR, Forsting M, Bockisch A, Antoch G. Breast cancer staging in a single session: Whole-body PET/CT mammography. *J Nucl Med* 2008;49:1215–1222.
- Hipwell JH, Vavourakis V, Han L, Mertzaniadou T, Eiben B, Hawkes DJ. A review of biomechanically informed breast image registration. *Phys Med Biol* 2016;61:R1–R31.
- Hofvind S, Ursin G, Tretli S, Sebuodegard S, Moller B. Breast cancer mortality in participants of the Norwegian Breast Cancer Screening Program. *Cancer* 2013;119:3106–3112.
- Houssami N, Hayes DF. Review of preoperative magnetic resonance imaging (MRI) in breast cancer: Should MRI be performed on all women with newly diagnosed, early stage breast cancer? *CA Cancer J Clin* 2009;59:290–302.
- Houssami N, Irwig L, Simpson JM, McKessar M, Blome S, Noakes J. Sydney breast imaging accuracy study: Comparative sensitivity and specificity of mammography and sonography in young women with symptoms. *Am J Roentgenol* 2003;180:935–940.
- Humphrey LL, Helfand M, Chan BK, Woolf SH. Breast cancer screening: A summary of the evidence for the US Preventive Services Task Force. *Ann Intern Med* 2002;137:347–360.
- Itoh A, Ueno E, Tohno E, Kamma H, Takahashi H, Shiina T, Yamakawa M, Matsumura T. Breast disease: Clinical application of US elastography for diagnosis. *Radiology* 2006;239:341–350.
- Jia WR, Chai WM, Tang L, Wang Y, Fei XC, Han BS, Chen M. Three-dimensional contrast enhanced ultrasound score and dynamic contrast-enhanced magnetic resonance imaging score in evaluating breast tumor angiogenesis: Correlation with biological factors. *Eur J Radiol* 2014; 83:1098–1105.
- Jiang YX, Liu H, Liu JB, Zhu QL, Sun Q, Chang XY. Breast tumor size assessment: Comparison of conventional ultrasound and

- contrast-enhanced ultrasound. *Ultrasound Med Biol* 2007;33:1873–1881.
- Jung EM, Jungius KP, Rupp N, Gallegos M, Ritter G, Lenhart M, Clevert DA, Kubale R. Contrast enhanced harmonic ultrasound for differentiating breast tumors—first results. *Clin Hemorheol Microcirc* 2005; 33:109–120.
- Jung HK, Kuzmiak CM, Kim KW, Choi NM, Kim HJ, Langman EL, Yoon S, Steen D, Zeng D, Gao F. Potential use of American College of Radiology BI-RADS mammography atlas for reporting and assessing lesions detected on dedicated breast CT imaging: Preliminary study. *Acad Radiol* 2017a;doi:10.1016/j.acra.2017.06.003.
- Jung I, Kim MJ, Moon HJ, Yoon JH, Kim EK. Ultrasonography-guided 14-gauge core biopsy of the breast: Results of 7 years of experience. *Ultrasonography* 2017b;doi:10.14366/usg.17028.
- Kalinyak JE, Berg WA, Schilling K, Madsen KS, Narayanan D, Tartar M. Breast cancer detection using high-resolution breast PET compared to whole-body PET or PET/CT. *Eur J Nucl Med Mol Imaging* 2014;41:260–275.
- Kalinyak JE, Schilling K, Berg WA, Narayanan D, Mayberry JP, Rai R, Dupree EB, Shusterman DK, Gittleman MA, Luo W, Matthews CG. PET-guided breast biopsy. *Breast J* 2011;17:143–151.
- Kalles V, Zografos GC, Provatopoulou X, Koulouchi D, Gounaris A. The current status of positron emission mammography in breast cancer diagnosis. *Breast Cancer* 2013;20:123–130.
- Kaplan SS. Automated whole breast ultrasound. *Radiol Clin North Am* 2014;52:539–546.
- Kelly KM, Dean J, Lee SJ, Comulada WS. Breast cancer detection: Radiologists' performance using mammography with and without automated whole-breast ultrasound. *Eur Radiol* 2010;20:2557–2564.
- Kelly KM, Richwald GA. Automated whole-breast ultrasound: Advancing the performance of breast cancer screening. *Semin Ultrasound CT MR* 2011;32:273–280.
- Keranen AK, Haapea M, Rissanen T. Ultrasonography as a guiding method in breast micro-calcification vacuum-assisted biopsies. *Ultraschall Med* 2016;37:497–502.
- Kerlikowske K, Grady D, Barclay J, Sickles EA, Ernster V. Effect of age, breast density, and family history on the sensitivity of first screening mammography. *JAMA* 1996;276:33–38.
- Kim EA, Yoon KH, Lee YH, Kim HW, Juhng SK, Won JJ. Focal hepatic lesions: Contrast-enhancement patterns at pulse-inversion harmonic US using a microbubble contrast agent. *Korean J Radiol* 2003;4: 224–233.
- Kim YJ, Kim SH, Jeh SK, Choi JJ, Kang BJ, Song BJ. Gel pad application for automated breast sonography. *J Ultrasound Med* 2015; 34:713–719.
- Kisslo J, Firek B, Ota T, Kang DH, Fleishman CE, Stetten G, Li J, Ohazama CJ, Adams D, Landolfo C, Ryan T, von Ramm O. Real-time volumetric echocardiography: The technology and the possibilities. *Echocardiography* 2000;17:773–779.
- Kolb TM, Lichy J, Newhouse JH. Comparison of the performance of screening mammography, physical examination, and breast US and evaluation of factors that influence them: An analysis of 27,825 patient evaluations. *Radiology* 2002;225:165–175.
- Kousaka J, Nakano S, Ando T, Tetsuka R, Fujii K, Yoshida M, Shiomi-Mouri Y, Goto M, Imai Y, Imai T. Targeted sonography using an image fusion technique for evaluation of incidentally detected breast lesions on chest CT: A pilot study. *Breast Cancer* 2016;23:301–309.
- Krag DN, Anderson SJ, Julian TB, Brown AM, Harlow SP, Costantino JP, Ashikaga T, Weaver DL, Mamounas EP, Jalovec LM, Frazier TG, Noyes RD, Robidoux A, Scarth HM, Wolmark N. Sentinel-lymph-node resection compared with conventional axillary-lymph-node dissection in clinically node-negative patients with breast cancer: Overall survival findings from the NSABP B-32 randomised phase 3 trial. *Lancet Oncol* 2010;11:927–933.
- Kriege M, Brekelmans CT, Boetes C, Besnard PE, Zonderland HM, Obdeijn IM, Manoliu RA, Kok T, Peterse H, Tilanus-Linthorst MM, Muller SH, Meijer S, Oosterwijk JC, Beex LV, Tollenaar RA, de Koning HJ, Rutgers EJ, Klijn JG. Efficacy of MRI and mammography for breast-cancer screening in women with a familial or genetic predisposition. *N Engl J Med* 2004;351:427–437.
- Kuhl CK, Schmützler RK, Leutner CC, Kempe A, Wardelmann E, Hocke A, Maringa M, Pfeifer U, Krebs D, Schild HH. Breast MR imaging screening in 192 women proved or suspected to be carriers of a breast cancer susceptibility gene: Preliminary results. *Radiology* 2000;215: 267–279.
- Kuhl CK, Schrading S, Bieling HB, Wardelmann E, Leutner CC, Koenig R, Kuhn W, Schild HH. MRI for diagnosis of pure ductal carcinoma in situ: A prospective observational study. *Lancet* 2007;370:485–492.
- Kuhl CK, Schrading S, Leutner CC, Morakkabati-Spitz N, Wardelmann E, Fimmers R, Kuhn W, Schild HH. Mammography, breast ultrasound, and magnetic resonance imaging for surveillance of women at high familial risk for breast cancer. *J Clin Oncol* 2005;23:8469–8476.
- Kuzmiak CM, Cole EB, Zeng D, Tuttle LA, Steed D, Pisano ED. Dedicated three-dimensional breast computed tomography: Lesion characteristic perception by radiologists. *J Clin Imaging Sci* 2016; 6:14.
- Kvistad K, Rydland J, Smethurst H-B, Lundgren S, Fjøsne H, Haraldseth O. Axillary lymph node metastases in breast cancer: Preoperative detection with dynamic contrast-enhanced MRI. *Eur Radiol* 2000; 10:1464–1471.
- Lamuraglia M, Lassau N, Garbay JR, Mathieu MC, Rouzier R, Jaziri S, Roche A, Leclerc J. Doppler US with perfusion software and contrast medium injection in the early evaluation of radiofrequency in breast cancer recurrences: A prospective phase II study. *Eur J Radiol* 2005;56:376–381.
- Lashkari AE, Pak F, Firouzmand M. Full intelligent cancer classification of thermal breast images to assist physician in clinical diagnostic applications. *J Med Signals Sens* 2016;6:12–24.
- Leach MO, Boggis CR, Dixon AK, Easton DF, Eccles RA, Evans DG, Gilbert FJ, Griebsch I, Hoff RJ, Kessar P, Lakhani SR, Moss SM, Nerurkar A, Padhani AR, Pointon LJ, Thompson D, Warren RM. Screening with magnetic resonance imaging and mammography of a UK population at high familial risk of breast cancer: A prospective multicentre cohort study (MARIBS). *Lancet* 2005;365:1769–1778.
- Lee HJ, Kim EK, Kim MJ, Youk JH, Lee JY, Kang DR, Oh KK. Observer variability of Breast Imaging Reporting and Data System (BI-RADS) for breast ultrasound. *Eur J Radiol* 2008;65:293–298.
- Lee SH, Chang JM, Kim WH, Bae MS, Cho N, Yi A, Koo HR, Kim SJ, Kim JY, Moon WK. Differentiation of benign from malignant solid breast masses: Comparison of two-dimensional and three-dimensional shear-wave elastography. *Eur Radiol* 2013;23:1015–1026.
- Li DD, Guo LH, Xu HX, Liu C, Xu JM, Sun LP, Wu J, Liu BJ, Liu LN, Xu XH. Acoustic radiation force impulse elastography for differentiation of malignant and benign breast lesions: A meta-analysis. *Int J Clin Exp Med* 2015;8:4753.
- Li N, Jiang YX, Zhu QL, Zhang J, Dai Q, Liu H, Yang Q, Wang HY, Lai XJ, Sun Q. Accuracy of an automated breast volume ultrasound system for assessment of the pre-operative extent of pure ductal carcinoma in situ: Comparison with a conventional handheld ultrasound examination. *Ultrasound Med Biol* 2013;39:2255–2263.
- Liberman L, Feng TL, Dershaw DD, Morris EA, Abramson AF. US-guided core breast biopsy: Use and cost-effectiveness. *Radiology* 1998; 208:717–723.
- Lind P, Igerc I, Beyer T, Reinprecht P, Hausegger K. Advantages and limitations of FDG PET in the follow-up of breast cancer. *Eur J Nucl Med Mol Imaging* 2004;31(suppl 1):S125–S134.
- Lindfors KK, Boone JM, Nelson TR, Yang K, Kwan AL, Miller DF. Dedicated breast CT: Initial clinical experience. *Radiology* 2008; 246:725–733.
- Lindfors KK, Boone JM, Newell MS, D'Orsi CJ. Dedicated breast CT: The optimal cross sectional imaging solution? *Radiol Clin North Am* 2010;48:1043–1054.
- Liu H, Tan T, van Zelst J, Mann R, Karssemeijer N, Platel B. Incorporating texture features in a computer-aided breast lesion diagnosis

- system for automated three-dimensional breast ultrasound. *J Med Imaging (Bellingham)* 2014;1:024501.
- Mameri CS, Kemp C, Goldman SM, Sobral LA, Ajzen S. Impact of breast MRI on surgical treatment, axillary approach, and systemic therapy for breast cancer. *Breast J* 2008;14:236–244.
- Mandelson MT, Oestreicher N, Porter PL, White D, Finder CA, Taplin SH, White E. Breast density as a predictor of mammographic detection: Comparison of interval- and screen-detected cancers. *J Natl Cancer Inst* 2000;92:1081–1087.
- Mansel RE, Fallowfield L, Kissin M, Goyal A, Newcombe RG, Dixon JM, Yiangou C, Horgan K, Bundred N, Monypenny I, England D, Sibbering M, Abdullah TI, Barr L, Chetty U, Sinnett DH, Fleissig A, Clarke D, Ell PJ. Randomized multicenter trial of sentinel node biopsy versus standard axillary treatment in operable breast cancer: The ALMANAC Trial. *J Natl Cancer Inst* 2006;98:599–609.
- Meissnitzer M, Dershaw DD, Lee CH, Morris EA. Targeted ultrasound of the breast in women with abnormal MRI findings for whom biopsy has been recommended. *AJR Am J Roentgenol* 2009;193:1025–1029.
- Meng W, Zhang G, Wu C, Wu G, Song Y, Lu Z. Preliminary results of acoustic radiation force impulse (ARFI) ultrasound imaging of breast lesions. *Ultrasound Med Biol* 2011;37:1436–1443.
- Mi CR, He Y, Wang W. Proto-explore of ultrasound contrast agents injected subcutaneously for enhancement in sentinel lymph nodes of breast masses. *Chin J Ultrasonogr* 2010;19:970–973.
- Miller AB, Wall C, Baines CJ, Sun P, To T, Narod SA. Twenty five year follow-up for breast cancer incidence and mortality of the Canadian National Breast Screening Study: Randomised screening trial. *BMJ* 2014;348:g366.
- Moon WK, Lo CM, Chang JM, Huang CS, Chen JH, Chang RF. Computer-aided classification of breast masses using speckle features of automated breast ultrasound images. *Med Phys* 2012;39:6465–6473.
- Moorman A, Bourez R, Heijmans H, Kouwenhoven E. Axillary ultrasonography in breast cancer patients helps in identifying patients preoperatively with limited disease of the axilla. *Ann Surg Oncol* 2014;21:2904–2910.
- Morris EA, Liberman L, Ballon DJ, Robson M, Abramson AF, Heerdt A, Dershaw DD. MRI of occult breast carcinoma in a high-risk population. *AJR Am J Roentgenol* 2003;181:619–626.
- Moss SM, Cuckle H, Evans A, Johns L, Waller M, Bobrow L. Effect of mammographic screening from age 40 years on breast cancer mortality at 10 years' follow-up: A randomised controlled trial. *Lancet* 2006;368:2053–2060.
- Moy L, Elias K, Patel V, Lee J, Babb JS, Toth HK, Mercado CL. Is breast MRI helpful in the evaluation of inconclusive mammographic findings? *AJR Am J Roentgenol* 2009;193:986–993.
- Nagarajan MB, Huber MB, Schlossbauer T, Leinsinger G, Krol A, Wismuller A. Classification of small lesions in dynamic breast MRI: Eliminating the need for precise lesion segmentation through spatio-temporal analysis of contrast enhancement over time. *Mach Vis Appl* 2013;24:1371–1381.
- Naik AM, Fey J, Gemignani M, Heerdt A, Montgomery L, Petrek J, Port E, Sacchini V, Sclafani L, VanZee K, Wagman R, Borgen PI, Cody HS, III. The risk of axillary relapse after sentinel lymph node biopsy for breast cancer is comparable with that of axillary lymph node dissection: A follow-up study of 4008 procedures. *Ann Surg* 2004;240:462–468, discussion 68–71.
- Nakano S, Ando T, Tetsuka R, Fujii K, Yoshida M, Kousaka J, Shiomi-Mouri Y, Imai T, Fukutomi T, Ishiguchi T, Arai O. Reproducible surveillance breast ultrasound using an image fusion technique in a short-interval follow-up for BI-RADS 3 lesions: A pilot study. *Ultrasound Med Biol* 2014;40:1049–1057.
- Nakano S, Kousaka J, Fujii K, Yorozuya K, Yoshida M, Mouri Y, Akizuki M, Tetsuka R, Ando T, Fukutomi T, Oshima Y, Kimura J, Ishiguchi T, Arai O. Impact of real-time virtual sonography, a coordinated sonography and MRI system that uses an image fusion technique, on the sonographic evaluation of MRI-detected lesions of the breast in second-look sonography. *Breast Cancer Res Treat* 2012a;134:1179–1188.
- Nakano S, Yoshida M, Fujii K, Yorozuya K, Kousaka J, Mouri Y, Fukutomi T, Oshima Y, Kimura J, Ishiguchi T. Real-time virtual sonography, a coordinated sonography and MRI system that uses magnetic navigation, improves the sonographic identification of enhancing lesions on breast MRI. *Ultrasound Med Biol* 2012b;38:42–49.
- Nakano S, Yoshida M, Fujii K, Yorozuya K, Mouri Y, Kousaka J, Fukutomi T, Kimura J, Ishiguchi T, Ohno K, Mizumoto T, Harao M. Fusion of MRI and sonography image for breast cancer evaluation using real-time virtual sonography with magnetic navigation: First experience. *Jpn J Clin Oncol* 2009;39:552–559.
- Nelson HD, Tyne K, Naik A, Bougatsos C, Chan BK, Humphrey L. Screening for breast cancer: An update for the US Preventive Services Task Force. *Ann Intern Med* 2009;151:727–737.
- Nunes LW, Schnall MD, Orel SG, Hochman MG, Langlotz CP, Reynolds CA, Torosian MH. Breast MR imaging: Interpretation model. *Radiology* 1997;202:833–841.
- Nystrom L, Andersson I, Bjurstam N, Frisell J, Nordenskjold B, Rutqvist LE. Long-term effects of mammography screening: Updated overview of the Swedish randomised trials. *Lancet* 2002;359:909–919.
- Obdeijn IMA, Brouwers-Kuyper EM, Tilanus-Linthorst MM, Wiggers T, Oudkerk M. MR imaging-guided sonography followed by fine-needle aspiration cytology in occult carcinoma of the breast. *Am J Roentgenol* 2000;174:1079–1084.
- O'Connell A, Conover DL, Zhang Y, Seifert P, Logan-Young W, Lin CF, Sahler L, Ning R. Cone-beam CT for breast imaging: Radiation dose, breast coverage, and image quality. *AJR Am J Roentgenol* 2010;195:496–509.
- O'Connell AM, Irshad A, Nguyen MS. Breast ultrasonography. *Ultrasound Clin* 2013;8:109–116.
- O'Connell AM, Karellas A, Vedantham S. The potential role of dedicated 3-D breast CT as a diagnostic tool: Review and early clinical examples. *Breast J* 2014;20:592–605.
- Pace LE, Keating NL. A systematic assessment of benefits and risks to guide breast cancer screening decisions. *JAMA* 2014;311:1327–1335.
- Park VY, Kim MJ, Kim E-K, Moon HJ. Second-look US: How to find breast lesions with a suspicious MR imaging appearance. *Radiographics* 2013;33:1361–1375.
- Parker SH, Jobe WE, Dennis MA, Stavros AT, Johnson KK, Yakes WF, Truell JE, Price JG, Kortz AB, Clark DG. US-guided automated large-core breast biopsy. *Radiology* 1993;187:507–511.
- Peters NH, Borel Rinkes IH, Zuithoff NP, Mali WP, Moons KG, Peeters PH. Meta-analysis of MR imaging in the diagnosis of breast lesions. *Radiology* 2008;246:116–124.
- Piron CA, Causser P, Jong R, Shumak R, Plewes DB. A hybrid breast biopsy system combining ultrasound and MRI. *IEEE Trans Med Imaging* 2003;22:1100–1110.
- Piscaglia F, Nolsøe C, Dietrich CF, Cosgrove D, Gilja O, Bachmann Nielsen M, Albrecht T, Barozzi L, Bertolotto M, Catalano O. The EFSUMB guidelines and recommendations on the clinical practice of contrast enhanced ultrasound (CEUS): Update 2011 on non-hepatic applications. *Ultraschall Med* 2012;33:33.
- Pons EP, Azcon FM, Casas MC, Meca SM, Espona JL. Real-time MRI navigated US: Role in diagnosis and guided biopsy of incidental breast lesions and axillary lymph nodes detected on breast MRI but not on second look US. *Eur J Radiol* 2014;83:942–950.
- Reinikainen HT, Rissanen TJ, Piippo UK, Paivansalo MJ. Contribution of ultrasonography and fine-needle aspiration cytology to the differential diagnosis of palpable solid breast lesions. *Acta Radiol* 1999;40:383–389.
- Ricci P, Cantisani V, Ballesio L, Pagliara E, Sallusti E, Drudi FM, Trippa F, Calascibetta F, Erturk SM, Modesti M, Passariello R. Benign and malignant breast lesions: Efficacy of real time contrast-enhanced ultrasound vs. magnetic resonance imaging. *Ultraschall Med* 2007;28:57–62.
- Riedl CC, Slobod E, Jochelson M, Morrow M, Goldman DA, Gonen M, Weber WA, Ulaner GA. Retrospective analysis of ¹⁸F-FDG PET/CT for staging asymptomatic breast cancer patients younger than 40 years. *J Nucl Med* 2014;55:1578–1583.

- Roe SM, Mathews JA, Burns RP, Sumida MP, Craft P, Jr., Greer MS. Stereotactic and ultrasound core needle breast biopsy performed by surgeons. *Am J Surg* 1997;174:699–703, discussion 703–74.
- Saadatmand S, Obdeijn IM, Rutgers EJ, Oosterwijk JC, Tollenaar RA, Woldringh GH, Bergers E, Verhoef C, Heijnsdijk EA, Hoening MJ. Survival benefit in women with BRCA1 mutation or familial risk in the MRI screening study (MRISC). *Int J Cancer* 2015;137:1729–1738.
- Saarenmaa I, Salminen T, Geiger U, Heikkinen P, Hyvarinen S, Isola J, Kataja V, Kokko ML, Kokko R, Kumpulainen E, Karkkainen A, Pakkanen J, Peltonen P, Piironen A, Salo A, Talviala ML, Haka M. The effect of age and density of the breast on the sensitivity of breast cancer diagnostic by mammography and ultasonography. *Breast Cancer Res Treat* 2001;67:117–123.
- Sadigh G, Carlos RC, Neal CH, Dwamena BA. Ultrasonographic differentiation of malignant from benign breast lesions: A meta-analytic comparison of elasticity and BIRADS scoring. *Breast Cancer Res Treat* 2012;133:23–35.
- Sahiner B, Chan HP, Roubidoux MA, Hadjiiski LM, Helvie MA, Paramagul C, Bailey J, Nees AV, Blane C. Malignant and benign breast masses on 3-D US volumetric images: Effect of computer-aided diagnosis on radiologist accuracy. *Radiology* 2007;242:716–724.
- Sakamoto N, Tozaki M, Higa K, Abe S, Ozaki S, Fukuma E. False-negative ultrasound-guided vacuum-assisted biopsy of the breast: Difference with US-detected and MRI-detected lesions. *Breast Cancer* 2010;17:110–117.
- Samani A, Zubovits J, Plewes D. Elastic moduli of normal and pathological human breast tissues: An inversion-technique-based investigation of 169 samples. *Phys Med Biol* 2007;52:1565–1576.
- Sardanelli F, Podo F, D'Agnolo G, Verdecchia A, Santaquilani M, Musumeci R, Trecate G, Manoukian S, Morassut S, de Giacomi C, Federico M, Cortesi L, Corcione S, Cirillo S, Marra V, Cilotti A, Di Maggio C, Fausto A, Preda L, Zuiani C, Contegiacomo A, Orlacchio A, Calabrese M, Bonomo L, Di Cesare E, Tonutti M, Panizza P, Del Maschio A. Multicenter comparative multimodality surveillance of women at genetic-familial high risk for breast cancer (HIBCRIT study): Interim results. *Radiology* 2007;242:698–715.
- Sardanelli F, Podo F, Santoro F, Manoukian S, Bergonzi S, Trecate G, Vergnaghi D, Federico M, Cortesi L, Corcione S. Multicenter surveillance of women at high genetic breast cancer risk using mammography, ultrasonography, and contrast-enhanced magnetic resonance imaging (the high breast cancer risk italian 1 study): Final results. *Invest Radiol* 2011;46:94–105.
- Sarica O, Uluc F. Additional diagnostic value of MRI in patients with suspicious breast lesions based on ultrasound. *Br J Radiol* 2014;87:20140009.
- Saslow D, Boetes C, Burke W, Harms S, Leach MO, Lehman CD, Morris E, Pisano E, Schnall M, Sener S. American Cancer Society guidelines for breast screening with MRI as an adjunct to mammography. *CA Cancer J Clin* 2007;57:75–89.
- Scaperrotta G, Ferranti C, Costa C, Mariani L, Marchesini M, Suman L, Folini C, Bergonzi S. Role of sonoelastography in non-palpable breast lesions. *Eur Radiol* 2008;18:2381–2389.
- Shen S, Zhou Y, Xu Y, Zhang B, Duan X, Huang R, Li B, Shi Y, Shao Z, Liao H, Jiang J, Shen N, Zhang J, Yu C, Jiang H, Li S, Han S, Ma J, Sun Q. A multi-centre randomised trial comparing ultrasound vs mammography for screening breast cancer in high-risk Chinese women. *Br J Cancer* 2015;112:998–1004.
- Shin HJ, Kim HH, Cha JH. Current status of automated breast ultrasonography. *Ultrasonography* 2015;34:165–172.
- Shin HJ, Kim HH, Cha JH, Park JH, Lee KE, Kim JH. Automated ultrasound of the breast for diagnosis: Interobserver agreement on lesion detection and characterization. *AJR Am J Roentgenol* 2011;197:747–754.
- Siegel RL, Miller KD, Jemal A. Cancer statistics, 2015. *CA Cancer J Clin* 2015;65:5–29.
- Siegel RL, Miller KD, Jemal A. Cancer statistics, 2017. *CA Cancer J Clin* 2017;67:7–30.
- Sim Y, Vinnicombe S, Whelehan P, Thomson K, Evans A. Value of shear-wave elastography in the diagnosis of symptomatic invasive lobular breast cancer. *Clin Radiol* 2015;70:604–609.
- Skaane P, Sager EM, Olsen JB, Abdelnoor M, Berger A, Wolff PA, Kullmann G. Diagnostic value of ultrasonography in patients with palpable mammographically noncalcified breast tumors. *Acta Radiol* 1999;40:163–168.
- Skaane P, Skjorten F. Ultrasonographic evaluation of invasive lobular carcinoma. *Acta Radiol* 1999;40:369–375.
- Skerl K, Vinnicombe S, Thomson K, McLean D, Giannotti E, Evans A. Anisotropy of solid breast lesions in 2-D shear wave elastography is an indicator of malignancy. *Acad Radiol* 2016;23:53–61.
- Smith WL, Surry KJ, Mills GR, Downey DB, Fenster A. Three-dimensional ultrasound-guided core needle breast biopsy. *Ultrasound Med Biol* 2001;27:1025–1034.
- Son JH, Jung HK, Song JW, Baek HJ, Doo KW, Kim W, Kim YM, Kim WW, Lee JS, Cho EY. Incidentally detected breast lesions on chest CT with US correlation: A pictorial essay. *Diagn Interv Radiol* 2016;22:514–518.
- Song SE, Seo BK, Cho KR, Woo OH, Son GS, Kim C, Cho SB, Kwon SS. Computer-aided detection (CAD) system for breast MRI in assessment of local tumor extent, nodal status, and multifocality of invasive breast cancers: Preliminary study. *Cancer Imaging* 2015;15:1.
- Spick C, Baltzer PA. Diagnostic utility of second-look US for breast lesions identified at MR imaging: Systematic review and meta-analysis. *Radiology* 2014;273:401–409.
- Sridharan A, Eisenbrey JR, Machado P, Ojeda-Fournier H, Wilkes A, Sevrakov A, Mattrey RF, Wallace K, Chalek CL, Thomenius KE, Forsberg F. Quantitative analysis of vascular heterogeneity in breast lesions using contrast-enhanced 3-D harmonic and subharmonic ultrasound imaging. *IEEE Trans Ultrason Ferroelectr Freq Control* 2015;62:502–510.
- Stacey-Clear A, McCarthy KA, Hall DA, Pile-Spellman E, White G, Hulka CA, Whitman GJ, Halpern EF, Kopans DB. Mammographically detected breast cancer: Location in women under 50 years old. *Radiology* 1993;186:677–680.
- Stavros AT, Thickman D, Rapp CL, Dennis MA, Parker SH, Sisney GA. Solid breast nodules: Use of sonography to distinguish between benign and malignant lesions. *Radiology* 1995;196:123–134.
- Stoblen F, Landt S, Stelkens-Gebhardt R, Sehoul J, Rezai M, Kummel S. First evaluation of the diagnostic accuracy of an automated 3-D ultrasound system in a breast screening setting. *Anticancer Res* 2011;31:2569–2574.
- Stomper PC, D'Souza DJ, DiNitto PA, Arredondo MA. Analysis of parenchymal density on mammograms in 1353 women 25–79 years old. *AJR Am J Roentgenol* 1996;167:1261–1265.
- Suga K, Yamamoto S, Tangoku A, Oka M, Kawakami Y, Matsunaga N. Breast sentinel lymph node navigation with three-dimensional interstitial multidetector-row computed tomographic lymphography. *Invest Radiol* 2005;40:336–342.
- Sugg SL, Ferguson DJ, Posner MC, Heimann R. Should internal mammary nodes be sampled in the sentinel lymph node era? *Ann Surg Oncol* 2000;7:188–192.
- Surry KJ, Mills GR, Bevan K, Downey DB, Fenster A. Stereotactic mammography imaging combined with 3 D US imaging for image guided breast biopsy. *Med Phys* 2007;34:4348–4358.
- Tan T, Mordang JJ, van Zelst J, Grivegnée A, Gubern-Mérida A, Melendez J, Mann RM, Zhang W, Platel B, Karssemeijer N. Computer-aided detection of breast cancers using Haar-like features in automated 3-D breast ultrasound. *Med Phys* 2015;42:1498–1504.
- Tan T, Platel B, Twellmann T, van Schie G, Mus R, Grivegnée A, Mann RM, Karssemeijer N. Evaluation of the effect of computer-aided classification of benign and malignant lesions on reader performance in automated three-dimensional breast ultrasound. *Acad Radiol* 2013;20:1381–1388.
- Tang AM, Kacher DF, Lam EY, Wong KK, Jolesz F, Yang ES. Simultaneous ultrasound and MRI system for breast biopsy: Compatibility assessment and demonstration in a dual modality phantom. *IEEE Trans Med Imaging* 2008;27:247–254.

- Tejerina Bernal A, Tejerina Bernal A, Rabadan Doreste F, De Lara Gonzalez A, Rosello Llerena JA, Tejerina Gomez A. Breast imaging: How we manage diagnostic technology at a multidisciplinary breast center. *J Oncol* 2012;2012:213421.
- Tilanus-Linthorst MM, Obdeijn IM, Bartels KC, de Koning HJ, Oudkerk M. First experiences in screening women at high risk for breast cancer with MR imaging. *Breast Cancer Res Treat* 2000;63:53–60.
- Torre LA, Bray F, Siegel RL, Ferlay J, Lortet-Tieulent J, Jemal A. Global cancer statistics, 2012. *CA Cancer J Clin* 2015;65:87–108.
- Tozaki M, Fukuma E. Category assessment based on 3 D volume data acquired by automated breast ultrasonography. *Jpn J Radiol* 2012;30:185–191.
- Tozaki M, Isobe S, Fukuma E. Preliminary study of ultrasonographic tissue quantification of the breast using the acoustic radiation force impulse (ARFI) technology. *Eur J Radiol* 2011;80:e182–e187.
- Uematsu T, Kasami M, Yuen S. Comparison of FDG PET and MRI for evaluating the tumor extent of breast cancer and the impact of FDG PET on the systemic staging and prognosis of patients who are candidates for breast-conserving therapy. *Breast Cancer* 2009;16:97–104.
- U.S. Food and Drug Administration (U.S. FDA). Medical devices: Somo-v Automated Breast Ultrasound System (ABUS): P110006 [Internet]. Silver Spring, MD: Author; 2012. Available at: <https://www.accessdata.fda.gov/scripts/cdrh/cfdocs/cfpma/pma.cfm?ID=P110006>. Accessed April 10, 2014.
- Valente SA, Levine GM, Silverstein MJ, Rayhanabad JA, Weng-Grumley JG, Ji L, Holmes DR, Spoto R, Sener SF. Accuracy of predicting axillary lymph node positivity by physical examination, mammography, ultrasonography, and magnetic resonance imaging. *Ann Surg Oncol* 2012;19:1825–1830.
- Vallone P, D'Angelo R, Filice S, Petrosino T, Rinaldo M, De Chiara A, Gallipoli A. Color-doppler using contrast medium in evaluating the response to neoadjuvant treatment in patients with locally advanced breast carcinoma. *Anticancer Res* 2005;25:595–599.
- Vedantham S, Karellas A, Emmons MM, Moss LJ, Hussain S, Baker SP. Dedicated breast CT: Geometric design considerations to maximize posterior breast coverage. *Phys Med Biol* 2013a;58:4099–4118.
- Vedantham S, Shi L, Karellas A, O'Connell AM, Conover DL. Personalized estimates of radiation dose from dedicated breast CT in a diagnostic population and comparison with diagnostic mammography. *Phys Med Biol* 2013b;58:7921–7936.
- Venkatesh SS, Levenback BJ, Sultan LR, Bouzghar G, Sehgal CM. Going beyond a first reader: A machine learning methodology for optimizing cost and performance in breast ultrasound diagnosis. *Ultrasound Med Biol* 2015;41:3148–3162.
- Veronesi U, Paganelli G, Viale G, Luini A, Zurrada S, Galimberti V, Intra M, Veronesi P, Robertson C, Maisonneuve P, Renne G, De Cicco C, De Lucia F, Gennari R. A randomized comparison of sentinel-node biopsy with routine axillary dissection in breast cancer. *N Engl J Med* 2003;349:546–553.
- Wan CF, Du J, Fang H, Li FH, Zhu JS, Liu Q. Enhancement patterns and parameters of breast cancers at contrast-enhanced US: Correlation with prognostic factors. *Radiology* 2012;262:450–459.
- Wang HY, Jiang YX, Zhu QL, Zhang J, Dai Q, Liu H, Lai XJ, Sun Q. Differentiation of benign and malignant breast lesions: A comparison between automatically generated breast volume scans and handheld ultrasound examinations. *Eur J Radiol* 2012;81:3190–3200.
- Wang Y, Wang W, Li J, Tang J. Gray-scale contrast-enhanced ultrasonography of sentinel lymph nodes in a metastatic breast cancer model. *Acad Radiol* 2009;16:957–962.
- Warner E, Messersmith H, Causer P, Eisen A, Shumak R, Plewes D. Systematic review: Using magnetic resonance imaging to screen women at high risk for breast cancer. *Ann Intern Med* 2008;148:671–679.
- Warner E, Plewes DB, Hill KA, Causer PA, Zubovits JT, Jong RA, Cutrara MR, DeBoer G, Yaffe MJ, Messner SJ, Meschino WS, Piron CA, Narod SA. Surveillance of BRCA1 and BRCA2 mutation carriers with magnetic resonance imaging, ultrasound, mammography, and clinical breast examination. *JAMA* 2004;292:1317–1325.
- Warner E, Plewes DB, Shumak RS, Catzavelos GC, Di Prospero LS, Yaffe MJ, Goel V, Ramsay E, Chart PL, Cole DE, Taylor GA, Cutrara M, Samuels TH, Murphy JP, Murphy JM, Narod SA. Comparison of breast magnetic resonance imaging, mammography, and ultrasound for surveillance of women at high risk for hereditary breast cancer. *J Clin Oncol* 2001;19:3524–3531.
- Watermann DO, Foldi M, Hanjalic-Beck A, Hasenburger A, Lughausen A, Prompeler H, Gitsch G, Stickeler E. Three-dimensional ultrasound for the assessment of breast lesions. *Ultrasound Obstet Gynecol* 2005;25:592–598.
- Weinreb JC, Newstead G. MR imaging of the breast. *Radiology* 1995;196:593–610.
- Wenkel E, Heckmann M, Heinrich M, Schwab SA, Uder M, Schulz-Wendtland R, Bautz WA, Janka R. Automated breast ultrasound: Lesion detection and BI-RADS classification—A pilot study. *Rofo* 2008;180:804–808.
- Wienbeck S, Fischer U, Perske C, Wienke A, Meyer HJ, Lotz J, Surov A. Cone-beam breast computed tomography: CT density does not reflect proliferation potential and receptor expression of breast carcinoma. *Transl Oncol* 2017a;10:599–603.
- Wienbeck S, Lotz J, Fischer U. Review of clinical studies and first clinical experiences with a commercially available cone-beam breast CT in Europe. *Clin Imaging* 2017b;42:50–59.
- Wojcinski S, Gyapong S, Farrokh A, Soergel P, Hillemanns P, Degenhardt F. Diagnostic performance and inter-observer concordance in lesion detection with the automated breast volume scanner (ABVS). *BMC Med Imaging* 2013;13:36.
- Xin L, Chen L, Zhang H, Liu Q, Xu L, Wang B, Li T, Duan X, Liu Y. [Analysis of detecting value of ultrasound and the clinic-pathological features of axillary metastasis in breast cancer]. *Zhonghua Wai Ke Za Zhi* 2014;52:924–928.
- Yamamoto S, Maeda N, Tamesa M, Nagashima Y, Suga K, Oka M. Sentinel lymph node detection in breast cancer patients by real-time virtual sonography constructed with three-dimensional computed tomography–lymphography. *Breast J* 2010;16:4–8.
- Yamamoto S, Maeda N, Tamesa M, Nagashima Y, Yoshimura K, Oka M. Prospective ultrasonographic prediction of sentinel lymph node metastasis by real-time virtual sonography constructed with three-dimensional computed tomography–lymphography in breast cancer patients. *Breast Cancer* 2012;19:77–82.
- Zhang X, Wu F, Han P. The role of ¹⁸F-FDG PET/CT in the diagnosis of breast cancer and lymph nodes metastases and micrometastases may be limited. *Hell J Nucl Med* 2014;17:177–183.
- Zhang YN, Wang CJ, Xu Y, Zhu QL, Zhou YD, Zhang J, Mao F, Jiang YX, Sun Q. Sensitivity, specificity and accuracy of ultrasound in diagnosis of breast cancer metastasis to the axillary lymph nodes in Chinese patients. *Ultrasound Med Biol* 2015;41:1835–1841.
- Zhao H, Xu R, Ouyang Q, Chen L, Dong B, Huihua Y. Contrast-enhanced ultrasound is helpful in the differentiation of malignant and benign breast lesions. *Eur J Radiol* 2010;73:288–293.
- Zhong LY, Li RZ, Cao ZM, Wu JH. The value of ultrasound contrast agents injected subcutaneously for diagnosing sentinel lymph nodes of breast cancer. *Chin J Ultrasonogr* 2007;16:770–772.